THESIS FOR THE DEGREE OF DOCTOR OF PHILOSOPHY

Unraveling the molecular mechanisms of herpes simplex virus attachment and release using cell membrane mimics

NADIA PEERBOOM

CHALMERS

Department of Physics
CHALMERS UNIVERSITY OF TECHNOLOGY
Göteborg, Sweden 2018

Unraveling the molecular mechanisms of herpes simplex virus attachment and release using cell membrane mimics

NADIA PEERBOOM
ISBN 978-91-7597-742-3

Doktorsavhandlingar vid Chalmers Tekniska Högskola
Ny serie nr 4423
ISSN 0346-718X

Department of Physics
Chalmers University of Technology
SE-412 96 Göteborg
Sweden
Telephone +46(0)31 - 772 10 00

Printed at Chalmers Reproservice
Göteborg, Sweden 2018

Cover illustration: *Artistic representation of the initial attachment of a virus to the plasma membrane of its host cell (Svenja Classen, 2018).*

Unraveling the molecular mechanisms of herpes simplex virus attachment and release using cell membrane mimics

NADIA PEERBOOM
Department of Physics
Chalmers University of Technology

Abstract

The herpes simplex virus is a widespread human pathogen, most commonly known for causing cold sores. Its infection cycle is initiated with the formation of multiple bonds between viral glycoproteins and cellular glycosaminoglycans, which are long polysaccharide chains found close to the cell surface. While the key molecular actors of this initial attachment have been identified, less is known about the dynamics of the herpes-glycosaminoglycan interaction.

This thesis focuses on implementing bioanalytical assays to address two main research questions. First, we investigated how specific physicochemical properties of the glycosaminoglycan chains and of the viral glycoproteins influence the binding characteristics of the virus, in particular particle mobility and binding kinetics. Second, we aimed at elucidating how new progeny virus successfully releases from the cell membrane without getting trapped. To this end, we used two different cell membrane mimics. The first one consisted of end-grafted glycosaminoglycan chains, mimicking the native brush-like architecture of glycosaminoglycans, while the second one was obtained through incorporation of native membrane material into supported lipid bilayers. To study virus mobility and measure affinities and binding forces, we mainly used total internal reflection fluorescence microscopy in combination with single particle tracking, and atomic force microscopy.

Our results showed that the type of GAG or the glycosylation of the viral glycoproteins influence the diffusive behavior of herpes simplex virions, which we attributed to a change in binding forces of the herpes-glycosaminoglycan interaction. Furthermore, we suggest that a highly glycosylated region, called mucin-like region, found on certain glycoproteins balances the herpes-glycosaminoglycan interaction to ensure successful release.

Taken together, this thesis provides new insights into the mechanisms regulating attachment and release of the herpes simplex virus to and from the cell membrane, which could be of relevance to the development of new strategies in antiviral research.

Keywords: herpes simplex virus, glycosaminoglycans, total internal reflection fluorescence microscopy, single particle tracking, binding kinetics, atomic force microscopy

Acknowledgements

This thesis would not have been possible without the contribution, help, and support of many people, to whom I would like to express my sincere gratitude and appreciation.

Marta Bally, my main supervisor. Your presence, care, optimism, honesty, and impressive skill to correct text in a short period of time, have been invaluable to me. I am very grateful for the great opportunity you gave me, and everything I learned from you.

Fredrik Höök, co-supervisor and examiner of this thesis. Thank you for your guidance, feedback, and encouragements throughout the years.

Tomas Bergström, Edward Trybala, and Maria Johansson, the virus team from Sahlgrenska. I have truly enjoyed our regular meetings on the red sofa. Thanks for your valuable input to my work, for sharing ideas, as well as your enthusiasm for this fascinating field. Maria deserves special thanks for kindly preparing the virus material, and teaching me how to handle it.

All collaborators, for their great work which made all of this possible. Stephan Block, thanks for your very valuable input to the papers. The tracking clearly made this thesis more interesting. Noomi Altgärde, thanks for introducing me to the lab, our good talks and laughs. Hudson Pace, for always being there when your help is needed. Thanks for your encouragements, and for being an awesome lab-buddy. Eneas Schmidt, for your efforts in the lab, and staying so calm even when bilayers did not want to form. Martin Delguste, for your hospitality during my stay in Louvain-la-Neuve.

Olov Wahlsten, your valuable advice has helped me find my way through this academic jungle. Thanks for your friendship, your contagious laughter, your genuine determination to win beer-bets, and of course for proofreading this thesis.

The Biological Physics group, including its former members. This has been a great journey and I am very grateful that I got to share it with such creative, helpful, fun, and friendly colleagues, from which many have become very good friends. Thank you for all the good memories, the fika breaks, afterworks, group trips, and conferences. My office mates deserve special mention, for sharing chocolate, music, dance, laughter, and furniture.

My family and friends back home, for your support and frequent visits. Thanks to my parents for teaching me not to give up, and my sister Svenja for drawing the cover illustration for this thesis. Thanks to my family and friends in Sweden for making me feel at home here too; especially Stefan, for helping me reach my goals, and being such a great person to have by my side. I am looking forward to our next adventure!

Nadia Peerboom, Göteborg, May 2018

Appended papers

Paper I

Binding kinetics and lateral mobility of HSV-1 on end-grafted sulfated glycosaminoglycans
Nadia Peerboom, Stephan Block, Noomi Altgärde, Olov Wahlsten, Stephanie Möller, Matthias Schnabelrauch, Edward Trybala, Tomas Bergström, and Marta Bally

Biophysical Journal **113**, 1-12 (2017)

Paper II

Mucin-like region of herpes simplex virus type 1 attachment protein glycoprotein C (gC) modulates the virus-glycosaminoglycan interaction
Noomi Altgärde, Charlotta Eriksson, Nadia Peerboom, Tuan Phan-Xuan, Stephanie Möller, Matthias Schnabelrauch, Sofia Svedhem, Edward Trybala, Tomas Bergström, and Marta Bally

Journal of Biological Chemistry **290(35)**, 21473-21485 (2015)

Paper III

The mucin-like region of gC-1 regulates the binding strength and mobility of herpes simplex virus type 1 during initial attachment to glycosaminoglycans
Nadia Peerboom, Martin Delguste, Maria Johansson, Edward Trybala, Tomas Bergström, David Alsteens, and Marta Bally

In manuscript

Paper IV

Herpes simplex virus type 2 mucin-like glycoprotein mgG promotes virus release from the surface of infected cells
Edward Trybala, Nadia Peerboom, Beata Adamiak, Malgorzata Krzyzowska, Jan-Åke Liljeqvist, Marta Bally, and Tomas Bergström

Submitted

Paper V

Cell membrane derived platform to study virus binding kinetics and diffusion with single particle sensitivity
Nadia Peerboom*, Eneas Schmidt*, Edward Trybala, Stephan Block, Tomas Bergström, Hudson Pace, and Marta Bally

ACS Infectious Diseases (Article in press)

*Authors contributed equally

My contribution to the appended papers

Paper I

I planned and performed all experiments, analyzed the data, prepared the figures, and wrote the main part of the manuscript.

Paper II

I designed and planned the TIRFM experiments together with N.A.. I analyzed the TIRFM data, and wrote the corresponding methods section of the manuscript.

Paper III

I conceived and coordinated this study together with M.B.. I planned and performed the TIRFM experiments and the corresponding data analysis. I performed the AFM experiments together with M.D.. I prepared all the figures and wrote the manuscript.

Paper IV

I planned and performed the TIRFM experiments, analyzed the data, prepared the corresponding figures, and wrote the corresponding parts of the manuscript.

Paper V

I coordinated this study together with M.B., and designed and planned the experiments, which I carried out partially. I prepared all the figures and wrote the main part of the manuscript.

List of abbreviations

AFM	Atomic force microscopy
CHO	Chinese hamster ovary
CPP	Critical packing parameter
CS	Chondroitin sulfate
DNA	Deoxyribonucleic acid
ECM	Extracellular matrix
EFA	Equilibrium fluctuation analysis
FD	Force distance
FRAP	Fluorescence recovery after photobleaching
FRET	Förster resonance energy transfer
GAG	Glycosaminoglycan
GFP	Green fluorescent protein
GMK	Green monkey kidney
HA	Hyaluronic acid
HIV	Human immunodeficiency virus
HPV	Human papillomavirus
HS	Heparan sulfate
HSV	Herpes simplex virus
HSV-1	Herpes simplex virus type 1
HSV-2	Herpes simplex virus type 2
HVEM	Herpesvirus entry mediator
MSD	Mean squared displacement
NMV	Native membrane vesicle
nSLB	Native-like supported lipid bilayer
PFU	Plaque forming unit
RNA	Ribonucleic acid
SA	Streptavidin
sHA	Sulfated hyaluronic acid
SLB	Supported lipid bilayer
SPR	Surface plasmon resonance
SPT	Single particle tracking
STM	Scanning tunneling microscope
TGN	Trans Golgi network
TIR	Total internal reflection
TIRFM	Total internal reflection fluorescence microscopy

Contents

1

Introduction

"Nothing in life is to be feared, it is only to be understood." – Marie Curie

Virus is a term that we are all familiar with, inducing fear in most, and fascination in some. Originating from the Latin word for poison, the term *virus* is generally used since the early 18th century to refer to infectious agents*. The first evidence of the existence of viruses dates back to 1892, when biologist Dimitri Ivanovsky observed that crushed leaf extracts from diseased tobacco plants remained infectious after removal of bacteria and fungi via filtration. Thus, the infectious agent (later discovered to be the tobacco mosaic virus) had to be smaller than bacteria and fungi, the only infectious agents known at the time. Indeed, viruses are too small to be visible in an optical microscope, which is why the first images of viruses could only be obtained after the invention of the electron microscope in the 1930s.

Today, almost 5000 virus species have been described[1], which is probably only a small fraction of all existing viruses on earth. They are all around us, residing in water, soil, air, and of course inside their hosts, which are the organisms they infect. The majority of these viruses do not cause the damaging effects that they are mostly known for, sometimes residing within their hosts for a lifetime, without producing any apparent effects at all. Some viruses have even been suggested to be beneficial to their hosts, providing protection from other viral diseases or bacterial infections[2]. Yet the most known and, for obvious reasons, most studied viruses are the ones causing acute disease. Two recent viral outbreaks have again demonstrated the threat that viruses can present to human health, namely the Ebola virus outbreak in West Africa between 2014 and 2015, causing more than 10 000 deaths[3], and the Zika virus outbreak in the Americas and the Pacific in 2016.

A virus infection starts with the transmission of a number of virus particles between hosts. This transmission generally occurs via vectors (insects and ticks for example), via food and water, or directly from person to person (for example via coughing and sneezing, sexual

*Since the 1980s, the word virus is also used to describe a self-replicating malicious software (also called malware), due to its common trait with biological viruses, to replicate only within its host (machine).

contact, or contaminated objects). Once inside the host, the virus needs to replicate in order to secure its existence. For this purpose, it hijacks the replication machinery of cells to produce new copies of itself. These progeny virus particles (also called virions), then continue to infect new hosts. During the virus infection cycle the cell membrane, separating the inside from the outside of the cell, plays an essential role. It constitutes a physical barrier, which the virus needs to cross to gain access to the cellular machinery. To this end, viruses have adapted to target so-called attachment factors [4], which are molecules present on the outer cell surface, allowing the virus to bind to the cell membrane, which triggers a cascade of events eventually leading to cell entry. These attachment factors frequently consist of carbohydrate groups exposed on the cell surface or in the extracellular matrix [5]. Many viruses also engage with the cell membrane to release the new progeny virions from the cell, which requires the initial binding to the cell surface to be overcome to successfully liberate the virions. The biomolecular interactions between virus and cell membrane, regulating attachment and release, will be the central theme of this thesis.

This thesis focuses on the herpes simplex virus (HSV), which is a very widespread human virus, commonly known for causing cold sores [6]. Initial attachment of HSV to the cell membrane is known to occur via formation of multiple bonds between viral glycoproteins and sulfated glycosaminoglycans (GAGs) [7], which are long polysaccharide chains present at the cell surface and in the extracellular matrix. Despite the high frequency of HSV infections, the exact mechanisms regulating attachment and release remain poorly understood. In particular, very little is known about the dynamics of the HSV-GAG interaction, which needs to be reversible to, for example, allow the virus to travel through the extracellular matrix, and to successfully release from the surface of infected cells.

The main research aim of this thesis was to elucidate the molecular mechanisms regulating the interactions between HSV and the cell membrane. In particular, two main factors likely to influence the interaction characteristics were studied, namely the physicochemical properties of the GAG chains, such as GAG sulfation, as well as the glycosylation of the viral glycoproteins. Our strategy was to implement two different bioanalytical platforms, mimicking the architecture of the cell membrane, as complements to traditional cell-based assays. The first model platform consisted of GAG chains grafted in an end-on configuration to a sensor surface, thereby creating a controlled reaction environment to study HSV-GAG interactions. The second model was derived directly from native cell membranes, and therefore represented a more natural system, which includes the whole range of membrane components, without relying on the use of live cells. These models were used in combination with total internal reflection fluorescence microscopy (TIRFM) to measure HSV binding kinetics and mobility, surface plasmon resonance (SPR), to characterize the surface functionalization and measure binding kinetics, and atomic force microscopy (AFM), to measure binding forces of the HSV-GAG interaction.

The remainder of this thesis will be organized as follows: **Chapter 2** provides a background to the biology relevant to this work, while **chapter 3** introduces general biophysical concepts. **Chapter 4** consists of a short review over different common strategies to study

virus-cell membrane interactions. **Chapter 5** contains the theoretical background of the main experimental methods and techniques used in the appended papers. **Chapter 6** summarizes and discusses the main findings of the appended papers. Finally, **chapter 7** concludes this thesis with final reflections and an outlook.

2

Background in biology

"Biology is the study of complicated things that give the appearance of having been designed for a purpose." – Richard Dawkins

Understanding life, its nature, origin, and complexity has always been a central theme in biological sciences. The early beginnings of this discipline were motivated primarily by people's curiosity, together with the wish to prevent and treat disease. Over the course of many generations, humans have built a collective knowledge of living organisms, their structure, function, and evolution, which we still strive to deepen today. In particular the technological progress of the past centuries has led to remarkable advances in the field, and enabled investigations of biological processes at a wide range of length scales.

The first studies of the human body, such as the early investigations of human anatomy in ancient Egypt and Greece [8], were conducted at the meter scale. An important milestone to decrease the length scale of biological studies was the invention of the optical microscope in the 17th century, which allowed the direct observation of cells and bacteria in the micrometer range. Today, thanks to advanced high-resolution technologies, we can study biological processes at the nanometer scale. Here we find the macromolecules essential to all living organisms. Four classes of macromolecules have been defined as the fundamental building blocks of life [9]: *proteins*, carrying out a vast number of functions within organisms, including catalysis of vital chemical reactions, *carbohydrates*, used for example for energy storage, *lipids*, providing structure to cell membranes, and *nucleic acids*, responsible for storing, transmitting and expressing genetic information.

This thesis focuses on the nanometer range, which is the length scale of viruses and the cell membranes they interact with during infection. This chapter provides the biological background of the different actors in virus-cell membrane interactions. First, the cell membrane is introduced, with a focus on three of the fundamental building blocks: lipids, proteins, and carbohydrates. Then, the general structure of viruses and the viral replication cycle are presented. Finally, the last section is dedicated to the herpes simplex virus, and the current knowledge about its interactions with the cell membrane.

2.1 The cell membrane

The cell membrane, also known as plasma membrane, is an essential component of the cell. It separates the content of the cell from the outer environment and acts as a barrier that controls the passage of molecules in and out of the cell. The cell membrane is a dynamic and flexible structure, built up mainly from lipids and proteins (figure 2.2).

Membrane lipids are amphiphilic molecules. They consist of a hydrophilic (polar) head group and a hydrophobic (nonpolar) hydrocarbon tail domain. In order to minimize the contact between the hydrophobic region and the surrounding water molecules, lipids arrange into distinct supramolecular assemblies when placed into an aqueous environment at a high enough concentration. The structure of these assemblies depends on the geometry of the lipid molecules, often characterized by the critical packing parameter (CPP)[10;11] $v/a_0 l_c$, where v is the volume of the hydrocarbon tail domain, a_0 the cross-sectional head group area, and l_c the maximum effective length of the hydrocarbon chain. For a CPP close or equal to one, the lipid has a cylindrical geometry, and its preferred self-assembly structure is a double-layered sheet, called bilayer (figure 2.1), with the hydrophobic hydrocarbon chains sandwiched between the hydrophilic head groups. The ~ 5 nm thick lipid bilayer is the basic structure of the cell membrane, accounting for approximately half of the mass of most animal cell membranes[12]. The most abundant lipids in the cell membrane are the phospholipids, whose general structure consists of the hydrophilic head and two fatty acid tails (figure 2.1).

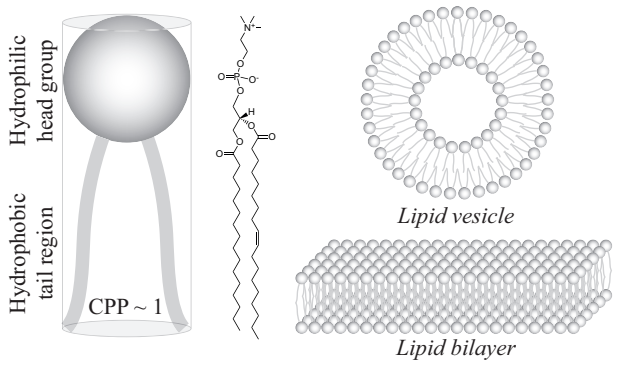

Figure 2.1: *Membrane lipids are amphiphilic molecules consisting of a hydrophilic head group and a hydrophobic tail region. The most abundant membrane lipid is the phospholipid, whose hydrophobic part comprises two fatty acid tails. The preferred self-assembly structure of the lipid depends on the critical packing parameter (CPP). A CCP close to one confers a cylindrical geometry to the lipid, resulting in lipid bilayer structures, such as the lipid vesicle or lipid bilayer.*

The remaining half of the membrane mass mainly comes from the membrane proteins that are responsible for most of the membrane's functions. These proteins are very diverse

in structure and in the way they are attached to the membrane. Some are covalently linked to the lipid bilayer and reside in the cytosol or in the extracellular matrix. So-called transmembrane proteins on the other hand are amphiphilic molecules and span across the whole membrane (with the hydrophobic parts being oriented towards the hydrocarbon tails of the lipids). The structure of a membrane protein is directly linked to its function. Transmembrane proteins are for example responsible for the transport of molecules across the membrane. Other proteins (both transmembrane proteins or proteins on the outer cell surface) serve as receptors for signaling molecules outside of the cell. The binding of a molecule to a receptor protein then usually results in a physiological response of the cell.

The concept of a fluid membrane was first introduced in the early 1970s by Singer and Nicolson, who proposed a so-called *fluid mosaic model* to describe biological membranes. According to this model, the cell membrane is a two-dimensional fluid, made of proteins embedded in a lipid matrix[13]. The concept of fluidity was of great importance for the understanding of the structure and functionality of biological membranes. Individual lipids can diffuse within the cell membrane with lateral diffusion coefficients on the order of $10^{-8}\,\mathrm{cm}^2/\mathrm{s}$[14]. The lateral diffusion of membrane proteins is very variable, but can be estimated to be around 1-5 orders of magnitude slower than membrane lipid diffusion[15].

Singer's and Nicolson's model turned out to be too simplistic and was therefore refined in 1982, when Karnovski *et al.* demonstrated that lipid molecules are, despite their lateral mobility, not homogeneously distributed in the membrane. They suggested that lipids form tightly packed microdomains within the membrane, thus creating heterogeneous structures of high significance for the functionality of the membrane[16]. For example, microdomains rich in sphingolipids and cholesterol, commonly referred to as membrane rafts, have been suggested to be involved in a wide range of processes, such as cell signaling, host-pathogen interactions, and a variety of disease conditions[17–19]. Although their existence still remains a controversy[20], membrane rafts could play an important role during viral infection, as viruses could exploit these domains as gateways for successful cell entry or exit[21;22].

2.2 Carbohydrates

Carbohydrates, also referred to as glycans or sugars, are the third building block of cells. They are one of the major components of the extracellular matrix (ECM), a layer of extracellular macromolecules extending from the membrane and surrounding all eukaryotic cells. Carbohydrates are also found attached to the cell membrane, all-together forming the *glycocalyx*, a layer of high complexity, which plays a key role during the cell's interactions with its surroundings. Unlike proteins, carbohydrates are not coded for in the cellular DNA, but are synthesized by the cell via enzymatic reactions. An interesting characteristic of carbohydrates is that they reflect certain disease states of the cell. For this reason, carbohydrates can be used as biomarkers for certain physiological conditions[23].

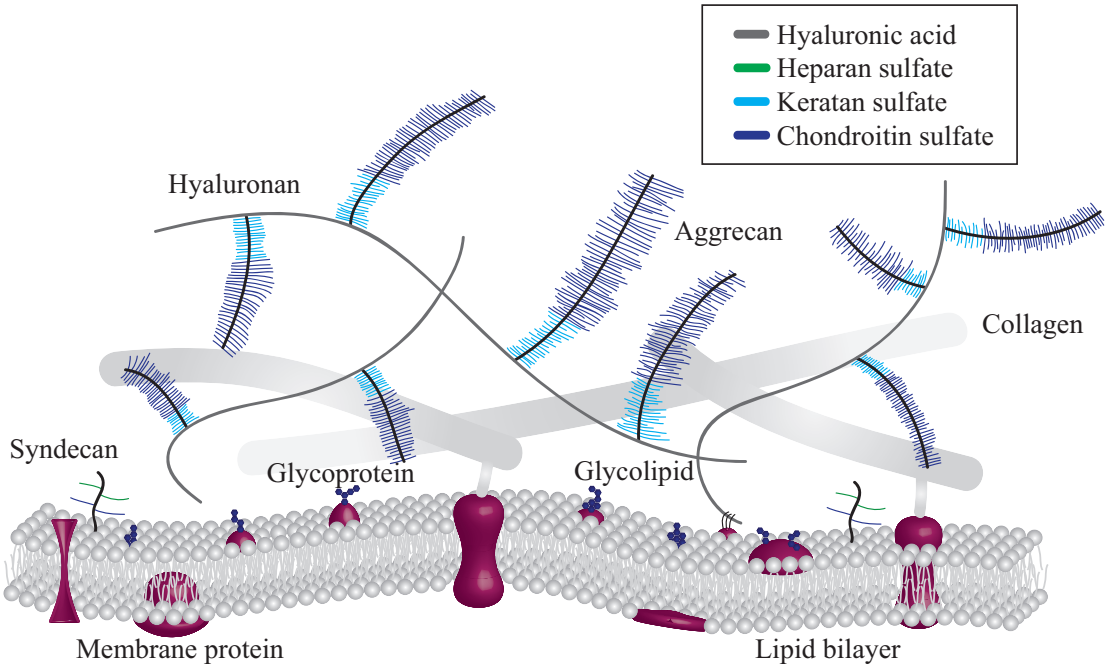

Figure 2.2: *Illustration of the cell membrane containing lipids and proteins, together with the extracellular matrix, displaying collagen, proteoglycans and glycosaminoglycans.*

Carbohydrates exist in different forms (figure 2.2): They can be attached to proteins, lipids, or secreted freely into the extracellular space. The addition of one or more monosaccharide units to a protein or lipid is called glycosylation[24]. This process confers additional information, structure and function to these molecules. More than half of all proteins are glycosylated[24]; they are then called glycoproteins. The carbohydrate groups on these proteins are either *N*-linked or *O*-linked, depending on the element the sugar unit is linked to (nitrogen or oxygen). Glycolipids, which are glycosylated lipids, represent 1% of all lipids found in a generic mammalian cell[25]. The head group of these lipids is formed by the monosaccharide units, meaning that the glycans are oriented towards the ECM. The most abundant glycolipids in mammalian cells are glycosphingolipids. They play a role in cell-cell recognition, cell surface reception, and messaging[25]. Some carbohydrates occur as long, unbranched polysaccharide chains, composed of repeating disaccharide units. These chains are either attached to a protein core (called a proteoglycan) or secreted freely into the ECM.

The glycan structures that we will focus the most on in this thesis are the *glycosaminoglycans* (GAGs). They are the main form of polysaccharides in mammalian cells. These long linear sugar chains are found both at the cell surface and in the extracellular matrix, therefore often serving as receptor sites for diverse biomolecules and pathogens. They also modulate cell adhesion, differentiation, migration, and proliferation[25]. Despite their structure made from repeating units of disaccharides (figure 2.3), GAGs are highly heterogeneous molecules. This is due to postsynthetic modifications of the chain, which mainly

consist of an addition of sulfate groups. The sulfation patterns on the GAG chains have been shown to be specific for certain tissues, development stages of the cell, and disease conditions[26;27]. As we will discuss later, the sulfation motifs on the chain ("sulfation code" of the GAG) also influence the interactions with viruses[28]. In this work, we focus on three different types of GAGs: hyaluronic acid/hyaluronan (HA), heparan sulfate (HS), and chondroitin sulfate (CS). HA is not sulfated and therefore has the simplest chemical composition. With up to 10 000 disaccharide units, it is by far the longest GAG that exists. Unlike HS and CS, HA is not bound to a protein core. HS and CS are made of 10 to 100 disaccharide units[29]. They differ in their disaccharide units, their sulfation patterns and their location in the ECM or on the cell surface. HS is mainly found attached to membrane proteoglycans (for example perlecan, agrin and syndecan). Syndecan also carries CS chains. In contrast, around 100 CS chains are covalently bound, in a brush-like configuration, to the proteoglycan aggrecan, present in the ECM and thus located further away from the cell membrane[30] (figure 2.2).

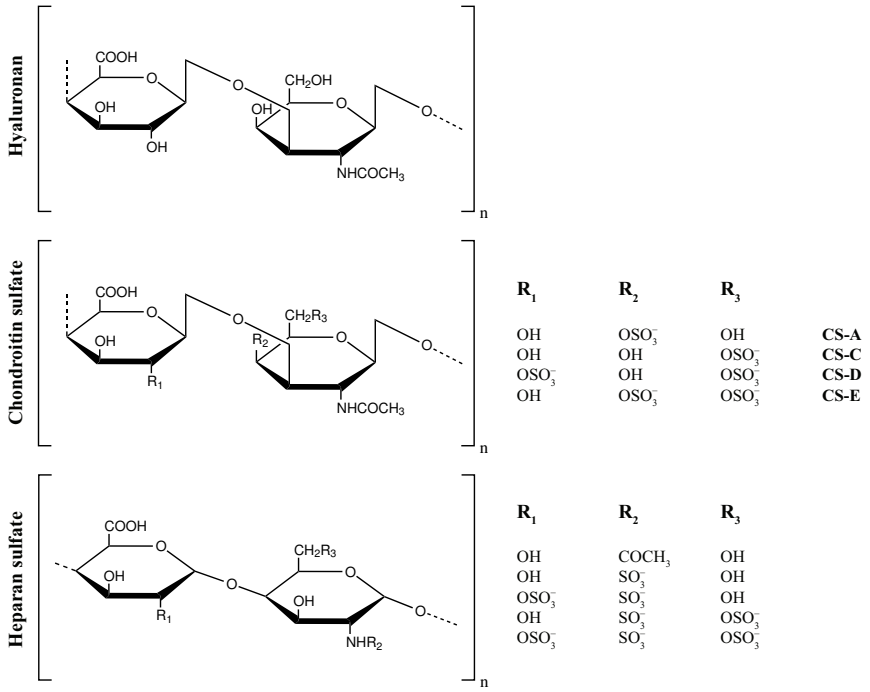

Figure 2.3: *Molecular structure of glycosaminoglycans used in this thesis work: hyaluronan, chondroitin sulfate, and heparan sulfate.*

As already mentioned, glycoconjugates often serve as attachment factors for viruses[31]. For example, a variety of viruses, such as influenza, take advantage of sialic acid residues on the cell surface for initial attachment[32]. Another important class of viruses bind to GAGs. Well-known examples are the human immunodeficiency virus (HIV)[33], the Ebola virus[34], the Zika virus[35], the human papillomavirus (HPV)[36], and the herpes simplex virus (HSV)[7]. The sulfation code of the GAGs and their location in the ECM play an important role in this binding process, as we will discuss further in this thesis.

2.3 Viruses

A virus is by its simplest definition a small infectious agent that uses the cell's replication machinery to produce new copies of itself. It can infect all species found on earth, from animal cells, to plant cells and bacteria. The diameter of a single virus particle, called virion, is in the nanometer range, with the smallest virus being around 20 nm (parvovirus). So-called superviruses can have characteristic diameters up to half a micrometer: the largest known virus, the mimivirus, has a diameter of about 400 nm with 100 nm long filaments extending from the capsid [37;38].

The general structure of a virus consists of a protein shell (also called capsid) protecting the viral genome. The genome can be either DNA or RNA and both can be either single or double stranded. Some viruses are enveloped, which means that a lipid membrane surrounds the protein capsid. This membrane is derived either from the plasma membrane of its host cell or obtained from one of the inner membranes of the cell. The viral lipid envelope embeds one or more species of proteins involved in different stages of the virus replication cycle, notably virus attachment, entry and release. These proteins are often glycosylated, therefore commonly referred to as glycoproteins.

Although viruses are generally not considered to be living organisms because of their incapacity to reproduce autonomously, their continued existence requires reproduction, just like for any living organism on earth. In order to reproduce, viruses infect host cells, which turn into virus-producing factories. The replication cycle of a virus (figure 2.4) is divided into different steps [38]: The first step is the attachment, during which viral proteins bind to specific attachment factors present on the cell surface. More viral proteins and cellular factors then come into play for successful virus entry into the cell. The virus enters the cell either by endocytosis (a process during which the plasma membrane bends around the virion and pinches off into the cytoplasm) or by fusion of the viral envelope with the cell membrane. Once inside the cell, the virus has to synthesize new viral components and replicate its genome. Synthesis of new components is done by transcription of the genetic information into messenger RNA, translation of this information into sequences of amino acids to form new proteins, and transport of viral components to different locations within the cell. Genome replication usually takes place in the cell nucleus but can also be carried out in the cytoplasm for certain viruses (most RNA viruses). Finally, the different viral components assemble to form new virions that exit the cell in the final step called egress. For enveloped viruses, egress can occur via budding at the plasma membrane, which is enriched with specific viral proteins. In this case, the virus acquires its viral envelope by deforming the membrane into a bud enveloping the rest of the viral components. Some viruses acquire their envelope by budding through the nuclear membrane. They are then transported out via vesicles that fuse with the plasma membrane. In certain types of infection cell lysis occurs to release the progeny virus.

How specific a viral infection is to the cell that is infected generally depends on the type of virus. A cell that can be infected by a certain type of virus and permit its replication

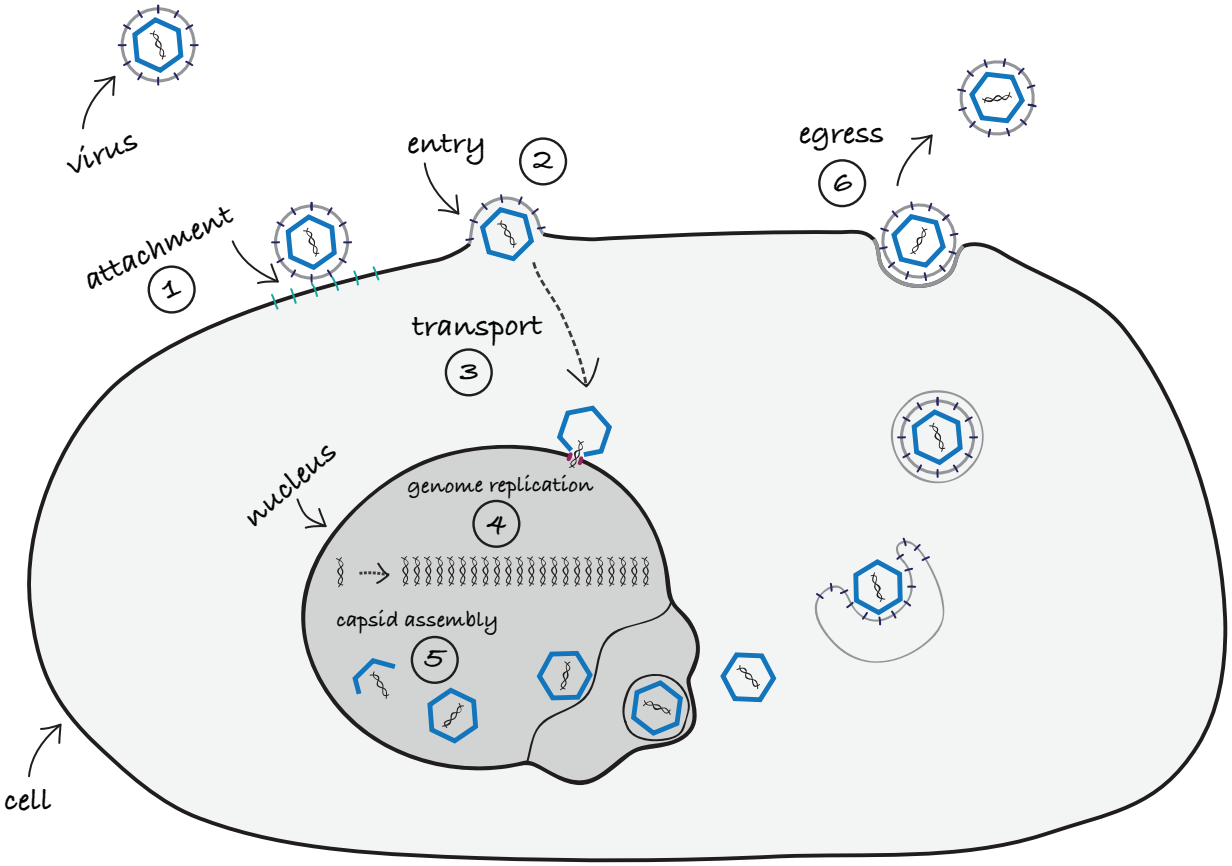

Figure 2.4: *Illustrative overview of the virus replication cycle based on the replication of the herpes simplex virus. After initial attachment to the cell membrane (1), the virus enters the cell (2) via endocytosis or fusion (as shown here). Viral components are transported to their respective replication sites (3). Genome replication (4) can take place either in the nucleus or in the cytoplasm. After assembly of the new viral components (5), the progeny virus leaves the cell in the final step called egress (6).*

is called a permissive cell. A permissive cells needs to meet a series of requirements for successful virus infection[38]: First of all the cell membrane must have attachment factors and entry receptors specific for that type of virus. Second, the cell must contain all the components necessary for virus replication (proteins and enzymes for example). This last requirement generally restricts the number of permissive cells for viruses with small genomes that almost entirely depend on the cell's replication machinery to copy their genome. Viruses with larger genomes are usually able to synthesize their own proteins and enzymes needed for the replication process inside the cell[37].

The fate of an infected cell depends on the type of virus infection, which can be divided into four groups[37]: Acute or lytic infections produce new virions at a high rate and result in rapid cell death. Persistent or chronic infections are long-term infections with a slow virus production. In latent or proviral infections, the viral genome resides in an inactive

state within the cell. Finally, in transforming infections, the cell's growth properties and phenotype are altered, which can for example lead to the development of cancer.

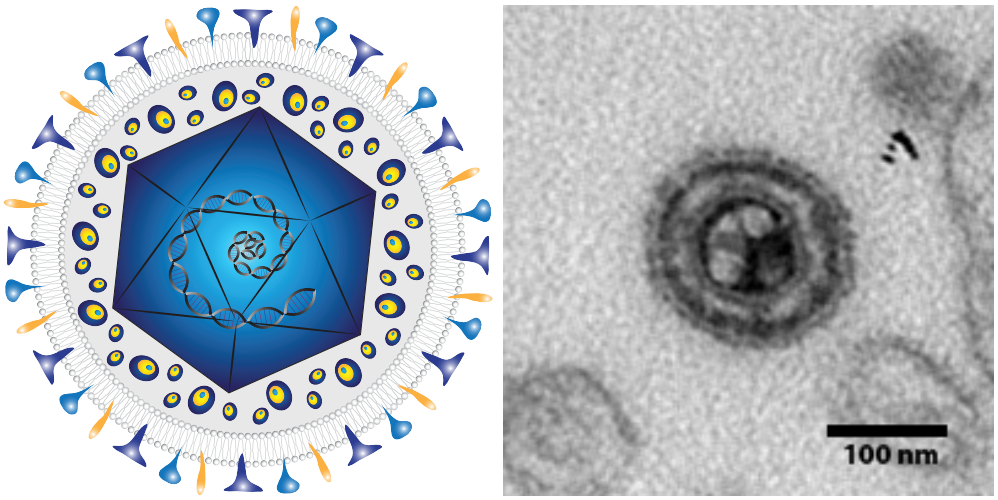

(a) (b)

Figure 2.5: *Herpes simplex virus.* ***(a)*** *Illustration showing the structure of HSV: The viral DNA is protected by an icosahedral protein cage, called capsid. The capsid is surrounded by a lipid envelope carrying the glycoproteins. The tegument, a cluster of proteins, fills the space between capsid and envelope.* ***(b)*** *Electron microscopy image of HSV-1 KOSc. Image acquired by Edward Trybala and Sibylle Widehn.*

2.4 The herpes simplex virus

The *herpes simplex virus* (HSV) belongs to the herpesvirus family (also called *herpesviridae*), which is characterized by large enveloped DNA viruses. The herpesvirus family can be divided into three subfamilies: *alphaherpesviruses* (including herpes simplex virus type 1 (HSV-1), herpes simplex virus type 2 (HSV-2), and the varicella zoster virus), *betaherpesviruses* (including the cytomegalovirus, and human herpesvirus 6A, 6B and 7), and *gammaherpesviruses* (including the Epstein-Barr virus and Kaposi's sarcoma-associated herpesvirus). The name of this family of viruses originates from the Greek word *herpein*, which means to creep, referring to the common characteristic of herpesviruses to cause life-long latent infections in their hosts [39].

This thesis focuses on the herpes simplex virus and its two serotypes HSV-1 and HSV-2. HSV is most commonly known for causing blisters on the skin or mucosa of the lips, mouth or genitals. While HSV-1 and HSV-2 preferentially reactivate from oral and genital sites respectively, both serotypes are able to infect either site [40]. HSV-1 is the more common infection (67% of the world population under the age of 50 is estimated to be infected [41]),

and primary infection often occurs during childhood (through contact with saliva or breast milk). HSV-2 being transmitted mainly via sexual contact, primary infection usually occurs later in life. For HSV-2, 11% of the world population aged 15-49 is estimated to be infected[41]. Both serotypes can cause lytic infections in fibroblasts and epithelial cells of the affected areas (oral or genital sites), and establish latency in neuron cells from which they can periodically reactivate.

HSV is an enveloped virus with a double-stranded DNA genome (figure 2.5a) enclosed by the protein capsid. With around 150 kilo base pairs[42;43], the genome of HSV is relatively large, which means that it encodes for a large number of different proteins. The viral envelope embeds twelve different species of glycoproteins, which all play a specific role in one or several virus replication steps[44]. The linker between capsid and envelope is the tegument, a cluster of proteins common to all herpesviruses.

Virus attachment is mediated by glycoproteins gC and gB binding to cell surface heparan sulfate (HS) and chondroitin sulfate (CS). gC-1 (glycoprotein gC of serotype HSV-1) is the main attachment protein of HSV-1 and it binds to HS[45] and CS[46;47]. It is however not essential for successful cell infection, since it has been shown that gB-1 mediates binding for gC-1 deficient HSV-1 virions[48]. The situation is different for HSV-2, where gB-2 (glycoprotein gB of HSV-2) has been suggested as the main attachment protein[49;50]. Virions that are deficient in both gC and gB show drastically reduced infectivity[48]. This has however been proposed to be partially due to the need of gB for viral entry[51]. Fusion between the viral envelope and the plasma membrane (figure 2.4) has been suggested as the main pathway for HSV entry into the cell[51]. It is triggered by glycoprotein gD (and additionally gB and gH/gL heterodimers) binding to entry receptors on the cell membrane. Three different classes of entry receptors have been identified[52]: HVEM (herpesvirus entry mediator), nectin-1 (both serotypes) and nectin-2 (HSV-2 only), as well as 3-*O*-sulfated HS (HSV-1 only). After fusion, the nucleocapsid (viral capsid containing the DNA) and tegument proteins are released into the cytoplasm of the host cell. An alternative pathway for viral entry via endocytosis and fusion at low pH with the endosomal membrane has been shown for HeLa and CHO cells[53], thus suggesting that HSV has two distinct pathways for viral entry, depending on the host cell. The nucleocapsid is transported to the cell nucleus where replication and transcription of the viral DNA, as well as assembly of the nucleocapsid takes place. To assemble a new virion a series of events follows[38](figure 2.4): First the nucleocapsid containing the viral DNA buds through the inner nuclear membrane, where it acquires a temporary envelope. This envelope then fuses with the outer nuclear membrane, releasing the nucleocapsid into the cytoplasm, where it gets coated with the tegument proteins. The capsid/tegument complex then acquires its final envelope by budding into a vesicle from the trans Golgi network (TGN), which expresses the glycoproteins. Finally, the TGN vesicle fuses with the plasma membrane to release the virion from the cell.

In this work, we focus on two key steps of the HSV replication cycle: the initial attachment of the virus to the cell membrane and the release of the progeny virions from the

cell membrane. These two processes are closely linked to each other: while the initial interactions between virus and cell membrane are essential to achieve viral entry, these same interactions must be overcome in order to ensure successful detachment of the newly produced virions from the cell membrane. Poor detachment would lead to trapping of the progeny virions on the surface of the infected cell, and result in a dead-end infection. To avoid trapping, the sialic acid binding influenza virus produces an enzyme (neuraminidase) that degrades sialic acid moieties on the cell surface, thereby facilitating virion release[54]. A similar mechanism, based on the HS degrading enzyme heparanase, has recently been suggested for HSV-1[55]. Hadigal *et al.* indeed demonstrated that HS expression on the cell surface is drastically decreased after HSV-1 infection and that this effect is a result of an upregulation of active heparanase upon infection. It is interesting to note that the genome of the influenza virus encodes for its receptor degrading enzyme neuraminidase, while HSV is not known to encode for any enzymes, but would take advantage of a host-enzyme to facilitate viral egress.

In this thesis we will discuss an alternative mechanism for regulation of attachment and release of HSV, related to the glycosylation of the viral glycoproteins. Viral glycoproteins are synthesized and glycosylated by the host cell machinery. Accordingly, the glycan structures found on the virus envelope are similar to those of cellular glycoproteins, consisting of *N*-linked or *O*-linked oligosaccharides[56]. It has been suggested that viruses take advantage of this similarity to protect themselves from the host's immune response, based on the idea that viral antigens, strongly resembling cellular structures, are more easily tolerated by the immune system[57;58]. HSV, among others, has been found to present regions of numerous clustered *O*-linked glycans on certain glycoproteins, structurally resembling the glycosylation of mucins. These so-called mucin-like regions form extended structures, comprising multiple negatively charged sialic acid residues, and covering substantial parts of the underlying and neighboring proteins. Therefore, mucin-like domains have been suggested to shield viral binding sites from unwanted or premature interactions. In **paper II** and **paper III** we investigate the role of a mucin-like region found close to the GAG-binding site on gC-1[59], which has been shown to affect binding kinetics of gC-1 to immobilized HS[60]. A similar structure has also been found on glycoprotein gG of HSV-2. **Paper IV** discusses its potential role in viral egress.

3

Concepts in biophysics

"Nothing happens until something moves." – Albert Einstein

Nature is governed by universal laws of physics. Four different fundamental forces have been identified to rule over everything that surrounds us. For example, lightning strikes during thunderstorms are caused by electrostatic forces emerging between positively and negatively charged regions in a cloud, and apples falling from trees are believed to have inspired Newton to formulate the theory of gravitation. The fundamental forces apply to the very big scales, describing the movement of planets and galaxies for example, but also to the very small scales, explaining how the nucleus of an atom holds together.

In the same way that atoms and planets obey the laws of physics, living matter does too. In fact, all processes regulating life are ruled by physics (entropy, for example, plays a particular role, which we will come back to soon). This highlights the importance and need of studying biological processes from a physicist's point of view.

This chapter aims to familiarize the reader with a few biophysical concepts of importance in this thesis work. We start with the basic concepts of thermodynamics and their importance in biology. We then discuss specificity and multivalency of receptor-ligand interactions and describe the formalism of binding kinetics. This is followed by a section dedicated to single particle diffusivity and tracking, a further topic of direct relevance to this thesis.

3.1 Thermodynamics

The cell is the fundamental unit of structure in all organisms. It is a very dynamic entity that is constantly changing. An equilibrium state, from a classical physics perspective, is therefore difficult to apply to any biological system. Nevertheless, the processes happening inside the cell occur at very different time scales, which makes it possible to consider isolated "quasiequilibrium" states ruled by the laws of thermodynamics [9].

Cells need to store and transform energy to be able to carry out vital reactions. The source of energy is food (fats, proteins, carbohydrates), or sunlight for plant or bacteria cells for example. During this process, the law of conservation of energy (first law of thermodynamics) has to be fulfilled. To help us describe the thermodynamic state of a cell, we need to introduce two important concepts, namely the concept of free energy minimization and the concept of entropy. The Gibbs free energy is defined as follows:

$$G = H - TS \tag{3.1}$$

The enthalpy H is the internal energy of the system and T is the temperature. S is the entropy of the system. It is a measure of the disorder of a system, or, more precisely, a measure of the number of microscopic configurations a system can exist in for a given macroscopic state[9]:

$$S = k_B \, lnW \tag{3.2}$$

where k_B is the Boltzmann constant and W is the number of microstates.

Every system strives for minimizing its free energy and an interaction takes place spontaneously only if $\Delta G < 0$. With this in mind, the equilibrium state of a biological system is defined as the macroscopic state, out of all possible states, which minimizes the Gibbs free energy. If we consider an isolated system (constant internal energy and mass), the minimization of the Gibbs free energy ($\Delta G < 0$) translates into a maximization of the entropy of the system ($\Delta S > 0$), which is known as the second law of thermodynamics. This implies, that the macroscopic equilibrium state of an isolated system will be the one that allows for the highest number of microscopic configurations.

One concept of great importance in biophysics, which can be explained by the second law of thermodynamics, is the hydrophobic effect[9]. When placing a nonpolar molecule in water, the water molecules in the vicinity of the nonpolar molecule are restricted in their formation of hydrogen bonds. The number of microscopic configurations of these water molecules, and thus the total entropy of the system, is thereby reduced. To minimize this entropy loss, nonpolar molecules tend to aggregate or phase separate when placed in water. This is known as the hydrophobic effect. It explains, for example, why water and oil do not mix, the arrangement of lipids into well-defined structures such as micelles or bilayers, as well as protein folding.

3.2 Intermolecular interactions

As we discussed earlier, there are four known fundamental forces, also called fundamental interactions. Each of them acts over a characteristic range. For example, the electromagnetic and the gravitational forces have a long range of action, which consequently makes

them apparent at our (human) scale. In contrast, the strong and weak interactions are short-range interactions, acting over a distance of approximately 10^{-15} m. Although invisible to the human eye, they are indispensable, as they become predominant at the length scale of elementary particles.

The forces that emerge between atoms (belonging to the same or to two different molecules) can be of different nature depending on the physical properties of the atoms (charge and polarity for example) and the interatomic distance. The strongest intermolecular (or intramolecular) interactions are the covalent bond and the electrostatic force. The covalent bond is a chemical bond formed by the sharing of electrons between atoms with a strength of $100 - 300\ \mathrm{k_BT}$ per bond, and a range of $0.1 - 0.2$ nm[10]. The electrostatic force, or Coulomb interaction as it can also be referred to, is a physical force emerging between two charged atoms. The strength of this interaction is on the order of $200\ \mathrm{k_BT}$ for monovalent ions such as Na^+ and Cl^- [10]. One fundamental difference between the covalent bond and the electrostatic force is the directionality of the interaction. The covalent bond is a directional force, meaning that the molecules orient themselves in well-defined angles relative to each other. The electrostatic force on the other hand is non-directional and therefore less *specific* than the covalent bond[10]. Other examples of non-directional forces involved in intermolecular interactions are van der Waals forces, hydrophobic interactions, hydrogen bonds and electric dipole interactions[10].

Intermolecular forces occupy a central role in the context of this thesis, as they drive the biomolecular interactions occurring between different binding partners (for example viruses and cellular attachment factors) that we probed in the appended papers. When characterizing biomolecular interactions, one often refers to the specificity of the interaction, which is defined as the ability of that interaction to occur only between a biomolecule A and another biomolecule B. If A is also able to bind to a third biomolecule C, but prefers to bind to B, we talk about *selectivity* instead. High specificity can also be achieved for non-directional forces if the three-dimensional arrangement of the two binding partners is favorable to that interaction (figure 3.1a). This is for example the case for antibody/antigen interactions[61].

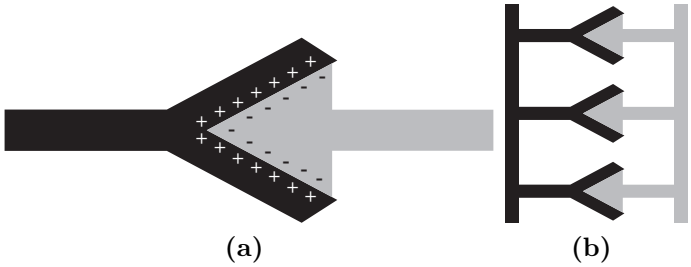

Figure 3.1: *Illustration of the concept of specificity and multivalency.* ***(a)*** *Non-directional forces can achieve high specificity if the three-dimensional arrangement is in favor of the interaction.* ***(b)*** *Multivalent interactions can be collectively stronger than the separate monovalent interactions they are composed of.*

Biomolecular interactions are often of *multivalent* nature, which means that they are created by simultaneous interactions between multiple binding sites on one entity and multiple binding sites on the other (figure 3.1b). This can lead to interactions that are collectively stronger and of higher selectivity than the monovalent interactions they are composed of[62]. Furthermore, the multivalent nature of an interaction could enhance the dynamics of certain biological processes, as several weak bonds can more easily be broken and reformed than a single bond of the same overall strength. Multivalency plays an important role in the context of recognition processes at the cell surface. Cell-to-cell adhesion, the attachment of bacteria to cells, and binding of extracellular vesicles are a few examples of multivalent interactions occurring at the cell surface[62;63], but it can be hypothesized that any molecule that comprises several binding sites relies on multivalency to interact with the cell membrane. The overall strength of such multivalent interactions is directly influenced by the number of bonds that are formed between the binding entity and the cell membrane, and can thus be related to the density and spatial arrangement of binding sites on the cell surface. For this reason, cells could benefit from multivalency to control the interactions the cell membrane engages into and protect the cell from undesired interactions.

Multivalency is a central concept in this thesis. Indeed, considering that viruses usually present several copies of binding proteins on their capsid or envelope, it is generally believed that the interaction between a virus and the cell membrane is of multivalent nature[62]. For example, multivalency has been studied for Simian virus 40[64–66], influenza[62], and HSV[67]. How exactly viruses take advantage of multivalency during attachment to the cell surface and entry remains to be further investigated. Nevertheless, it can be hypothesized that the formation of multiple bonds between the virus particle and the cell membrane confers stability and increased strength to the interaction, which could be a prerequisite for viral entry. Furthermore, because of a higher capacity of breaking and reforming bonds, viruses could use diffusive mechanisms to travel along the cell surface in search for suitable entry sites[68]. Finally, the formation of multiple bonds with the cell surface could trigger the deformation of the membrane, necessary for particle uptake[69].

3.3 Quantifying binding kinetics

Besides specificity, selectivity, and multivalency, biomolecular interactions are characterized by their *affinity*. The affinity is a measure of the strength of the interaction. It is related to the binding and unbinding rates (also called on and off rates, respectively) of the reaction describing the formation of a bound complex from two binding entities. The formalism to quantify these rates will be presented in this section.

We will first consider a simple interaction between one binding entity, herein called ligand L, and another one called receptor R, forming the complex LR. Since the assays used in this work are all based on the recognition of biomolecular interactions occurring close to a surface, we will focus here on the case of ligands in solution, binding to receptors

immobilized on a surface (figure 3.3a).

$$\mathrm{L} + \mathrm{R} \underset{k_{off}}{\overset{k_{on}}{\rightleftharpoons}} \mathrm{LR} \tag{3.3}$$

k_{on} and k_{off} are the reaction coefficients for binding and release respectively, also called association and dissociation rate constants. They can be related to the activation energies $\Delta E_{on/off}$ of association and dissociation respectively using the following expression:

$$k_{on/off} = A \ \exp\left(-\frac{\Delta E_{on/off}}{k_B T}\right) \tag{3.4}$$

T is the temperature of the system and A represents the number of collisions per unit time and concentration of ligands in the case of k_{on}, and the number of dissociation attempts per second for k_{off}. We define the equilibrium dissociation constant $K_D = k_{off}/k_{on}$, which is expressed in molar and has a low value for a high affinity interaction. It can be related to the Gibbs free energy (see figure 3.2):

$$K_D = k_{off}/k_{on} = A \ \exp\left(-\frac{\Delta E_{off} - \Delta E_{on}}{k_B T}\right) = A \ \exp\left(\frac{-\Delta G}{k_B T}\right) \tag{3.5}$$

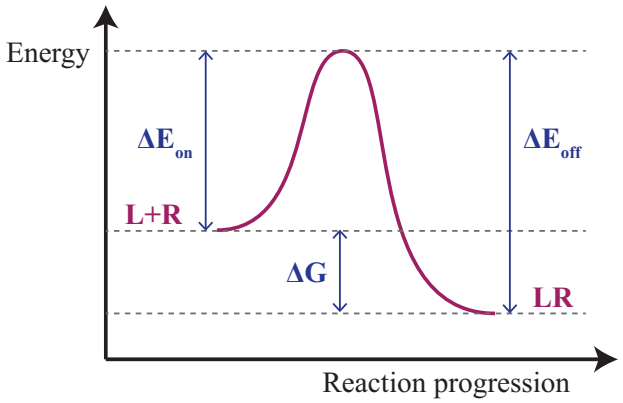

Figure 3.2: *Arrhenius plot: The reaction constants for association and dissociation can be related to the activation energies for both processes and thus to the Gibbs free energy according to equation* (3.4) *and* (3.5).

The rate of binding depends on two mechanisms: the rate of reaction, *i.e.* how fast the reaction between L and R occurs, and the diffusion of the ligand molecules in solution, *i.e.* the mass transport. One of these processes usually occurs much faster than the other, making one the limiting factor of the binding event. For this reason a system is either classified as reaction-limited or diffusion-limited (mass transport-limited) [70].

To quantify binding kinetics in a reaction-limited system, we consider the Langmuir model, which assumes fast diffusion and reversible binding (continual association and dissociation of ligands). The number of ligands bound to a receptor per unit area is given by $\Theta(t)$ and the rate of change is written as:

$$\frac{d\Theta(t)}{dt} = k_{on}C(\Theta_{max} - \Theta(t)) - k_{off}\Theta(t) \tag{3.6}$$

C is the concentration of ligands in solution and Θ_{max} is the total number of surface-bound receptors per unit area.

To solve this differential equation we consider two cases of different boundary conditions. The first case is association to an empty surface $\Theta(0) = 0$. The solution is then given by:

$$\Theta(t) = \frac{k_{on}C\Theta_{max}}{k_{on}C + k_{off}}[1 - \exp(-[k_{on}C + k_{off}]t)] \tag{3.7}$$

This expression is known as the Langmuir isotherm. At $t \to \infty$ equilibrium is reached, meaning that the rates of binding and release are equal. Equation (3.7) then becomes after rearrangement:

$$\frac{\Theta_{eq}}{\Theta_{max}} = \frac{C}{C + K_D} \tag{3.8}$$

For dissociation, the boundary condition becomes $\Theta(0) = \Theta_{eq}$ and we have $C = 0$. The solution of equation (3.6) is then expressed as an exponential decay:

$$\Theta(t) = \Theta_{eq}\exp(-k_{off}t) \tag{3.9}$$

The reaction in (3.3) describes a simple monovalent interaction of two binding molecules of equilibrium dissociation constant K_D^{mono}. If we consider n independent monovalent interactions, the total equilibrium dissociation constant is given by[62]:

$$K_D^{multi} = (K_D^{mono})^n \tag{3.10}$$

However, in the case of two multivalently interacting binding entities (forming n bonds), the individual interactions are not necessarily independent, but present a certain degree of *cooperativity* α. The concept of cooperativity was introduced to describe a situation where the formation of additional bonds is either facilitated or hindered by the creation of the first bond. $\alpha > 1$ indicates positive cooperativity, which means that each additional bond forms more easily than the previous one and the overall affinity (also called *avidity*) is

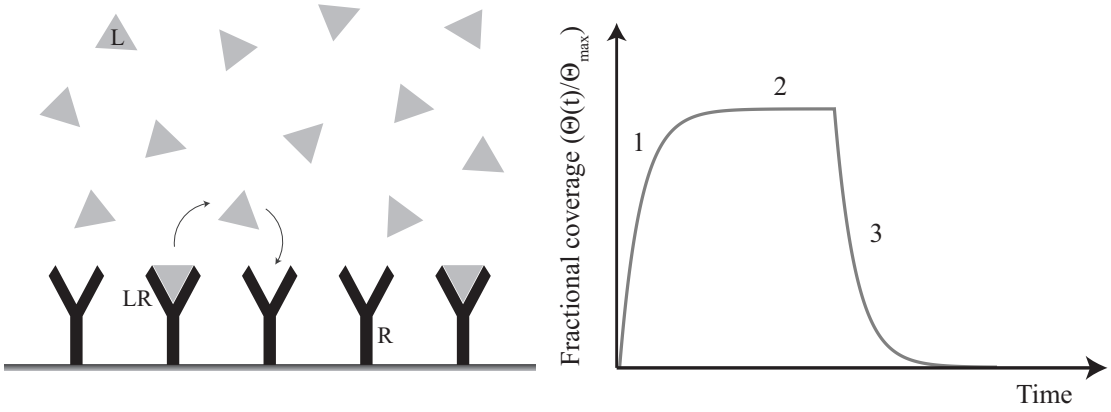

Figure 3.3: *Illustration of the Langmuir model.* ***(a)*** *Ligands in solution bind to and release from receptors immobilized on a surface.* ***(b)*** *The fractional coverage expressed as a function of time can be divided into three parts: 1. Association of ligands to surface-bound receptors 2. Equilibrium conditions (total rate of change is zero) 3. Exponential decay of bound ligands during rinsing step (no ligands in bulk solution).*

higher than in the case of independent bonds ($K_D^{multi} < (K_D^{mono})^n$). $\alpha < 1$ indicates negative cooperativity, for which $K_D^{multi} > (K_D^{mono})^n$. To account for cooperativity, equation (3.8) can be generalized to:

$$\frac{\Theta_{eq}}{\Theta_{max}} = \frac{C^\alpha}{C^\alpha + K_{0.5}^\alpha} \tag{3.11}$$

which is known as the Hill equation[71;72]. For $\alpha = 1$ (no cooperativity) $K_{0.5} = K_D$ (equations (3.8) and (3.11) become identical).

The Langmuir model (figure 3.3b) does not take into account the depletion of ligand molecules close to the surface. If ligand molecules diffuse slowly, this depletion zone is larger and the system is diffusion limited. In that case, the number of bound ligands per unit area is given by the Ilkovic equation[70]:

$$\Theta(t) = 2C_0\sqrt{\frac{Dt}{\pi}} \tag{3.12}$$

C_0 is the concentration of ligands in the bulk solution, and D represents their diffusion coefficient, as defined in section 3.4.

It is worth recalling that the rate of change in equation (3.6) includes both on and off rates. Techniques based on ensemble averaging (like surface plasmon resonance for example, described in chapter 5), can not dissect pure association and dissociation signals from

the overall binding curve. However, association and dissociation can be analyzed independently of each other using techniques capable of single particle detection. This is the case for equilibrium fluctuation analysis (EFA) [73], a method based on total internal reflection fluorescence microscopy (see chapter 5) that we used in this work. With this method, time-lapse movies of single particles interacting with the surface are analyzed. The software counts, for each frame, the number of newly bound and released particles, and determines the residence time of each individual particle. Association curves are generated directly from the cumulative plot of newly bound particles over time, while dissociation curves are constructed based on the individual residence times of the dissociated particles.

The slope of the association curve (also called association rate) generated by EFA is given by

$$\frac{dN_+}{dt} = k_{on}\ N_{fr}\ C \tag{3.13}$$

$N_{fr} = \Theta_{max} - \Theta(t)$ represents the number of free surface receptors per unit area. Equation (3.13) is derived from equation (3.6) after eliminating the negative release term. Assuming an excess of free surface receptors (*i.e.* $\Theta_{max} \gg \Theta(t)$ in equation (3.6)), we obtain:

$$\frac{dN_+}{dt} = k_{on}\ N_r\ C \tag{3.14}$$

where N_r is the total number of receptors on the surface per unit area (representing Θ_{max}). Equation (3.14) shows that the association rate is directly proportional to the association rate constant k_{on}.

The dissociation curve obtained from EFA can be written as:

$$N(t) = N_{eq} \exp(-k_{off} t) + N_{irr} \tag{3.15}$$

where N_{eq} represents the total number of associated particles per unit area, and N_{irr} the number of irreversibly bound particles per unit area.

3.4 Diffusivity and single particle tracking

When microscopic particles are suspended in a fluid, they move randomly in the solution. This movement is called *Brownian motion*, named after the botanist Robert Brown, who in 1827 observed pollen grains in water under a microscope and saw small particles randomly moving in the cavities of the pollen grain, filled with water. The underlying mechanism behind this motion was described 78 years later by Albert Einstein. He suggested that the observed random movement of suspended particles in solution is due to collisions with the

surrounding molecules of the solution[74]. The latter ones are in constant movement due to their thermal energy of the order of k_BT. The diffusion coefficient for the particles is given by the Stokes-Einstein equation*:

$$D = \frac{k_BT}{6\pi\eta r} \tag{3.16}$$

where η is the dynamic viscosity of the medium and r the hydrodynamic radius of the particle. As can be seen from this equation, the diffusion coefficient of the particle is directly related to its size. Measuring the diffusion coefficients of particles undergoing Brownian motion thus makes it possible to calculate their size distribution. Several techniques take advantage of this principle to determine the size distribution of nanoparticles in solution. One example is nanoparticle tracking analysis (NTA)[75].

In single particle tracking (SPT) the trajectories of individual particles are analyzed to extract information about diffusivity and type of motional behavior. This technique is often used in combination with fluorescence microscopy and based on the fact that the position of single fluorescent objects can be determined with a localization precision in the nanometer range, by applying a Gaussian fit to their intensity profiles[76]. SPT has been very popular to study the mobility of lipids and proteins in cell membranes, being an alternative to widely used ensemble averaging techniques, like fluorescence recovery after photobleaching (FRAP) for example†. A common approach in SPT analyses is to calculate the mean squared displacement (MSD) of the tracked particles. The MSD is a measure of the deviation of the particle position in relation to a reference position over time. It is defined as:

$$MSD(\Delta t) = \langle (x_{i+n} - x_i)^2 + (y_{i+n} - y_i)^2 \rangle \tag{3.17}$$

for $n = 1, 2, 3, \ldots, N$. The particle located in (x_i, y_i) will be at position (x_{i+n}, y_{i+n}) after n frames. $\Delta t = n\tau$ is called lag-time, where τ is the time between frames. N is an arbitrary number, but should in general be chosen smaller than one quarter of the total frame number to avoid falsification of MSD values at high lag-times due to too few data points[15]. An illustration of how the MSD is determined for a particle trajectory is shown in figure 3.4a.

For a particle performing a random walk in a two-dimensional plane the MSD curve is linear:

$$MSD(\Delta t) = 4D\Delta t \tag{3.18}$$

*The Stokes-Einstein equation is valid for fluids of low Reynolds number.

†In a FRAP experiment, a small region of a fluorescent sample is photobleached to measure the diffusion of molecules in and out of the bleached spot[77–79].

We then talk about normal diffusion and the diffusion coefficient is estimated from a linear fit of the MSD curve. Equation (3.18) can be generalized to account for anomalous diffusion, the case when the normal diffusion of the particle is hindered:

$$MSD(\Delta t) = 4D\Delta t^{\alpha} \tag{3.19}$$

where $\alpha = 1$ for normal diffusion and $\alpha < 1$ for anomalous diffusion.

For confined diffusion we observe an asymptotic MSD curve:

$$MSD(\Delta t) = A_c \left[1 - C_1 \exp\left(-\frac{4C_2 D\Delta t}{A_c}\right)\right] \tag{3.20}$$

A_c is the area of the confinement and the constants C_1 and C_2 are given by the geometry of the confinement. Finally, the MSD for diffusion under directed motion is given by:

$$MSD(\Delta t) = \nu^2\Delta t^2 + 4D\Delta t \tag{3.21}$$

where ν is the velocity of the directed motion. Figure 3.4b illustrates how the MSD curve is interpreted to classify the trajectories into the different types of diffusion.

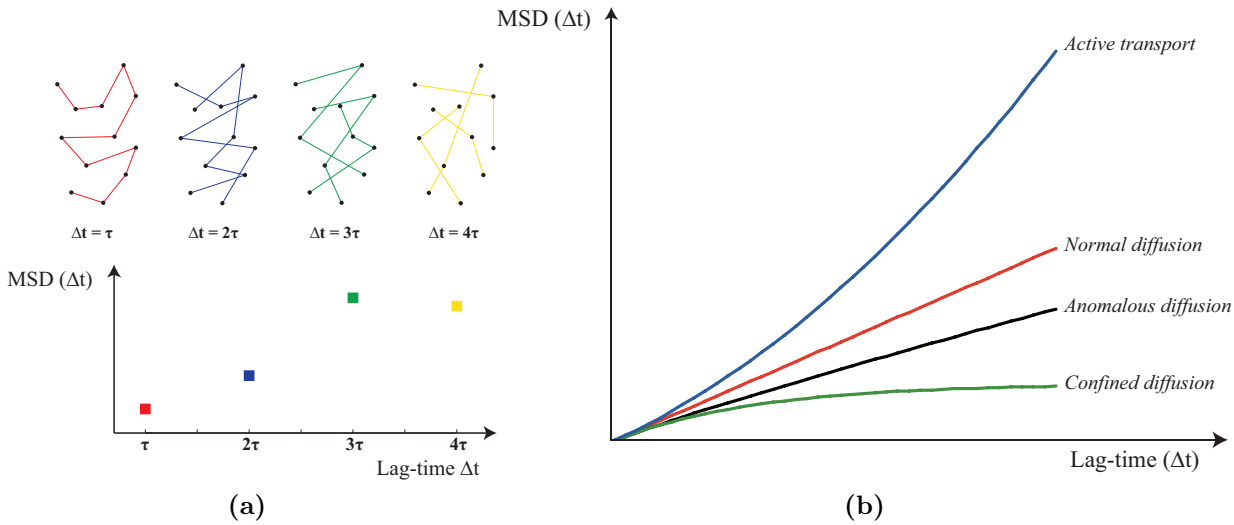

Figure 3.4: *Mean squared displacement (MSD), inspired from[80]. **(a)** Illustration of how an MSD curve is obtained for an arbitrary trajectory and $\Delta t = \tau, 2\tau, 3\tau, 4\tau$. **(b)** Different modes of diffusion (active transport, normal diffusion, anomalous diffusion, and confined diffusion) can be determined by the behavior of the MSD curve (see main text for corresponding equations).*

4

Strategies for probing virus-cell membrane interactions

"Everything should be made as simple as possible, but not simpler." – Albert Einstein

During the infection cycle, viruses encounter the cell membrane at multiple occasions. As described more in detail in chapter 2, an infection is initiated by the attachment of the virus to the cell membrane, and, for many types of infections, concludes with the release of progeny virus from the cell membrane. Therefore, the interactions occurring between viral binding proteins and cell membrane components play a key role during infection and are subject to a lot of attention in virus research. These efforts aim to develop a fundamental knowledge of virus-cell membrane interactions, with the ultimate goal to identify new antiviral compounds (targeting either viral or cellular binding molecules) that inhibit initial binding to the cell membrane or the release of progeny virus from the cell membrane.

This chapter reviews commonly used strategies to study virus-cell membrane interactions. The main focus of this chapter will be on surface-based methods, which recognize binding events between two entities of which one is attached to a surface. Such assays offer the possibility to focus exclusively on binding events between the virus (or viral binding proteins) and cell membrane components, without the contribution of other cellular factors. The complexity of the presented systems increases throughout the chapter, starting off with very simple systems involving only the two binding entities of interest, and moving towards complex native systems. Finally, a short section will be dedicated to solution-based systems, which do not require the presence of a surface for recognition of binding events.

4.1 From surface-immobilization of membrane receptors to artificial cell membrane mimics

Initial binding of viruses to the cell membrane occurs between specific viral binding proteins and cellular attachment factors and is followed by viral entry, which requires a strong attachment of the virus to so-called entry receptors. To characterize these specific interactions, a number of strategies have been developed to isolate the viral binding protein and cell membrane component of interest and measure their interaction kinetics using surface-based sensing. The most common approach of such methods is to attach the cell membrane component (herein called receptor) to the sensor surface (figure 4.1) and to add the viral protein (herein called ligand) to the solution that the surface is exposed to. This simple strategy has been used, for example, to extract information about binding kinetics for biomolecular interactions between viral glycoproteins and cell membrane attachment factors[81;82]. These receptor-based systems represent the most simplified approach to measure virus-cell membrane interactions. They make it possible to isolate the interaction of interest from other cellular processes occurring *in vivo*, and present a high degree of control and flexibility. For example, receptor density and physicochemical properties of the surface can easily be tuned to meet the needs of the experimenter. Furthermore, these systems are well-suited for inhibition studies that aim at testing new antiviral compounds targeting specific cell membrane or viral components[83;84]. A major challenge when working with receptor-based systems arises from the need to extract the membrane components of interest from their native environment, where they are usually present at very low levels. Common methods to purify membrane protein receptors, for example, rely on genetic overexpression[85] and detergent solubilization methods[86;87]. Receptor immobilization can be achieved in many different ways, mainly depending on the physicochemical properties of the substrate and the biomolecule to be immobilized. Common strategies include direct adsorption, covalent binding through amino groups, and affinity interactions between recognition pairs (*i.e.* biotin-avidin)[88;89]. Another challenge for these systems in particular, and surface-based methods in general, are non-specific interactions of ligands with the surface. Various surface passivation strategies have been developed to coat the surface with non-reactive compounds, thereby reducing levels of non-specific ligand adsorption. Which passivation agent to use usually depends on the type of substrate. Standard examples are Poly(L-lysine)-g-Poly(ethylene glycol) (PLL-g-PEG) or bovine serum albumin (BSA) coatings[90;91].

The simplicity of the above-described receptor-based systems, which offers advantages in terms of flexibility and control, also represents a major limitation. For example, it has been shown that certain cell membrane receptors, in particular membrane proteins, require their natural lipid environment to preserve their functionality[92;93]. Furthermore, certain viruses could rely on membrane receptor mobility to engage in multivalent interactions[94], which would be an important factor for studies involving whole virus particles. For this reason, many studies incorporate the purified membrane receptors in so-called

supported lipid bilayers (SLBs) (figure 4.1). SLBs are planar double-layered sheets of lipids formed on a support. SLBs can form spontaneously from lipid vesicles, which are spherical shells made of a lipid bilayer. When put in contact with the substrate, vesicles adsorb to it and, upon reaching a critical surface coverage, rupture to form an SLB [95;96]. This approach is one of the simplest to create SLBs. Another common method to form SLBs are deposition methods like the Langmuir-Blodgett method for example, which forms lipid films in a layer-by-layer approach by immersing the substrate into an aqueous solution exposing the lipid molecules at the air-solution interface [97]. The choice of substrate is critical for successful SLB formation. Indeed, spontaneous SLB formation via vesicle rupture has been shown for a limited number of materials only (mostly glass and other silica substrates [98]), and requires thorough cleaning procedures, which can challenge the reproducibility of SLB-based studies. SLBs represent two-dimensional fluids, in which the lipid molecules can diffuse freely. Therefore, a major advantage of these systems over simpler receptor immobilization-based systems is that the mobility of the incorporated membrane receptors can be preserved. Hence, SLB-based systems represent models of the cell membrane that are closer to the native cell membrane, while preserving the control and flexibility of the direct surface-immobilization approach. Furthermore, lipid bilayers have been shown to serve as a passivation layer, reducing non-specific interactions with the substrate [99]. SLB-based systems have been used, for example, to gain important insights into the kinetics and diffusion properties of virus-cell membrane interactions [64;66;100;101], as well as to study viral fusion [102;103].

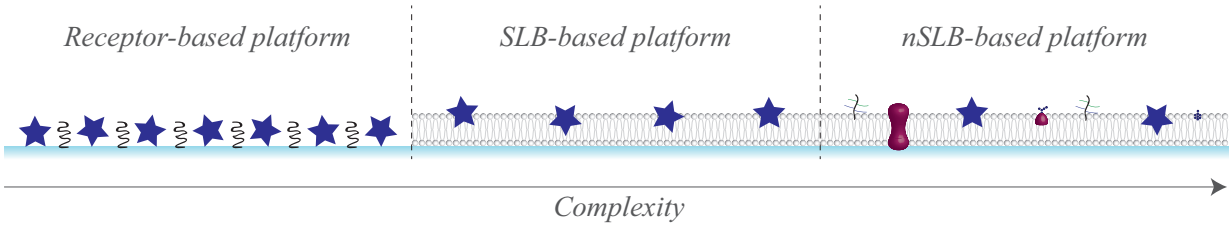

Figure 4.1: *Illustrations of three surface-based platforms to probe virus-cell membrane interactions described in this chapter. The first one is based on the immobilization of cell membrane receptors of interest to a sensing surface. In the second one the membrane receptors are embedded in a supported-lipid bilayer. In the third one SLBs are formed directly from native cell membrane material.*

4.2 Supported lipid bilayers from native cell membrane material

The previous section dealt with artificial systems commonly used to probe virus-cell membrane interactions, starting off with very simplified receptor-based systems and introducing SLBs as a means to better mimic the structure of the cell membrane and preserve protein

functionality and mobility. These SLBs can be tuned to increase in complexity, by incorporating, for example, different types of lipids, membrane proteins or other cell membrane molecules, such as cholesterol[104;105]. This approach of gradually increasing the complexity of the system can be viewed as a bottom-up design. As an alternative, using a top-down design, one starts from a very complex system and simplifies it to meet the needs of the experimental setup. In particular in this context, a top-down approach would be to form SLBs directly from native cell membrane material (figure 4.1). As compared to artificial SLBs, the composition of such native-like SLBs (nSLBs) is closer to native cell membranes, as they contain the whole range of membrane components (*e.g.* lipids, proteins, carbohydrates), without relying on detergent-based purification methods. nSLB systems fill the gap between simplified artificial systems and complex live-cell experiments: a combination of high compositional complexity and flexibility, compatible with surface-based methods, which isolates the membrane-related processes from other cellular factors.

Different methods can be used to extract native cell membrane material from cells and obtain so-called native membrane vesicles (NMVs). Two common methods are mechanical cell disruption and centrifugation[106;107], and cell blebbing[108;109]. While these extraction procedures can already bring about certain complications, the main challenge of nSLB-based systems lies in the formation of SLBs from NMVs, which contain high amounts of proteins, gel-phase lipids, and cholesterol, which have all been shown to impair spontaneous vesicle rupture[104;105;110;111]. A number of strategies have been developed to overcome this issue[112], including bilayer edge-induced vesicle fusion[113], α-helical (AH) peptide-induced vesicle fusion[105], co-adsorption of synthetic and native vesicles[109;114], formation of hybrid vesicles via sonication of synthetic and native vesicles[115], as well as the use of polyelectrolyte cushions to facilitate vesicle rupture[116].

To this day, only very few studies have used nSLB systems to probe virus-cell membrane interactions[117]. In **paper V** we implemented a platform based on the hybrid vesicle method[118] to measure binding kinetics and diffusion of single HSV-1 particles.

4.3 Viral cell-based assays

As stated above, the different systems presented in this chapter follow a trend of increasing complexity. For this reason, this section is dedicated to commonly used assays that involve whole cells, thereby offering the full range of cellular and viral factors to probe virus-cell membrane interactions. As we will discuss, the trade-off is a loss in control and flexibility as provided by the above described model systems. The assays described herein are of relevance to this thesis work and only represent a small fraction of the numerous cell-based assays used in virus research.

4.3.1 Viral plaque assay

A commonly used assay in virus research is the viral plaque assay[119;120]. It is used mainly to measure the infectivity of a virus suspension and determine the infectious dose. Such a plaque assay consists of preparing a dilution series (usually 10^x-fold dilutions) of the virus suspension and incubating a confluent dense monolayer of cells with the virus solution of a given dilution factor. Infected cells will produce new progeny virus and undergo morphological changes (for example due to cell lysis). To restrict the spread of the infection to neighboring cells only, a gel-like substance is usually added to the cell medium. A plaque will form at the infected area, which grows in size and, after a few days typically, becomes visible to the naked eye (figure 4.2). With a simple manual readout scheme, one then determines the number of plaque forming units (PFU) per milliliter of the initial virus suspension. Since the PFU count is a measure of the infectivity of the virus suspension, the viral plaque assay is a common method for testing anti-viral compounds. It is very versatile with respect to which step of the virus infection cycle the given compound targets, and has been used, for example, to evaluate the efficiency of binding inhibitors[121;122], *i.e.* compounds which prevent the virus from binding to the cell membrane. However, this assay does not isolate initial binding from the other steps of the viral infection cycle, like the assays based on cell membrane mimics described above did. Therefore it is not possible to distinguish between an impaired ability of the viruses to bind to the cell membrane, or, for example, to replicate within the cell.

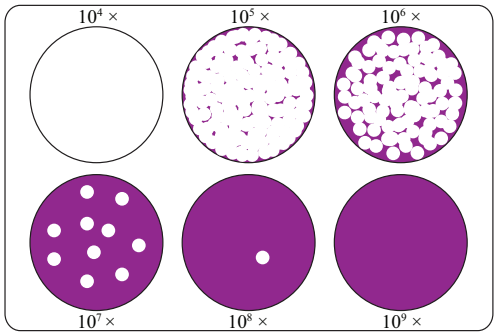

Figure 4.2: *Illustration of the viral plaque assay. Virus solutions of different dilution factors are added to a monolayer of cells to determine the level of infectivity of the viral suspension by counting the number of plaque forming units (PFU).*

4.3.2 Single-cell imaging

Single-cell imaging denotes a collection of microscopy techniques allowing the acquisition of images from individual cells. Examples of such microscopy techniques are electron microscopy and fluorescence microscopy. In virus research, such techniques can be used to observe, track and count viral particles engaging with the imaged cell. This is usually

achieved by attaching a fluorescent probe to the viral particle. In electron microscopy, a technique that was used in **paper II** & **IV**, the resolution of the images is high enough to detect single virus particles, and image their structure (figure 2.5b). Therefore the technique is well-suited to, for example, count the number of virions at the cell surface, which in **paper II** & **IV** allowed us to gain insights into the ability of certain HSV variants to release from the surface of the infected cell. However, electron microscopy is not compatible with live cells. For this reason, the infected cells are fixated prior to imaging, which does not make it possible to study dynamic processes.

To study the dynamic processes occurring on the cell surface during initial attachment, and prior to cell uptake, fluorescence microscopy techniques, such as total internal reflection fluorescence microscopy (introduced in chapter 5) or scanning confocal microscopy are commonly used[80;123], although studies using label-free techniques based on scattering have also been reported[124]. These high-resolution microscopy techniques are used in combination with single particle tracking to characterize the diffusive behavior of viruses on the cell surface, and inside the cell. In particular, live-cell SPT has been used for the observation and characterization of lateral mobility along the cell surface for a number of viruses, such as dengue virus[125;126], sindbis virus[127], influenza A[128], adenovirus type 2[129], murine polyomavirus[130] (study on virus-like particles), vaccinia virus[124], as well as bacteriophage lambda[68]. The biological significance of these observations will be further discussed in chapter 7. As compared to SPT studies on planar membrane systems, additional efforts are usually needed in live cell imaging to discern virus particles diffusing on the cell membrane from the ones in solution or within the cell. Also, the inherent movement of the cells can complicate the tracking analysis.

4.4 Solution-based assays

Most of the systems that were described in this chapter are surface-based. However, although not further explored in this thesis work, solution-based systems offer an alternative method to probe virus-cell membrane interactions without relying on the attachment of the studied membrane receptor to a sensor surface. This has the advantage of circumventing the difficulties related to non-specific surface interactions and to mimic a reaction environment that is more similar to the *in vivo* environment, where interaction partners are rarely static. Solution-based assays to probe virus-cell membrane interactions often rely on ensemble averaging, which means that they do not resolve single binding events but measure signals that originate from a collective of binding events. Such assays have for example been used to study fusion of enveloped viruses with liposomes[131;132]. Nevertheless, solution-based systems can also be combined with single particle approaches, as has been done, for example, to detect virus particles in solution[133].

5

Experimental methods

"I suppose it is tempting, if the only tool you have is a hammer, to treat everything as if it were a nail." – Abraham Maslow

Experimental strategies to probe virus-cell membrane interactions rely on two key elements. The first one is the biological system, which can either be a model of the cell membrane characterized by a certain level of compositional complexity, or whole cells in the case of cell-based assays, as discussed in the previous chapter. In this chapter we focus on the other key element, which is the experimental technique used to detect and characterize the biomolecular interactions between the virus (or viral glycoproteins) and the cell membrane. The main technique used in the context of this thesis to probe the interactions between HSV and cell membrane mimics is total internal reflection fluorescence microscopy (TIRFM), which is a surface-sensitive microscopy technique relying on the fluorescent labeling of the studied sample. In addition, we used atomic force microscopy (AFM), and surface plasmon resonance (SPR), which also both recognize biomolecular interactions occurring at a surface. TIRFM and AFM can both be used for single-particle studies, as they allow the recognition of single binding events. This is a major advantage when studying highly heterogeneous virus samples, which can contain subpopulations with very distinct physicochemical properties. SPR on the other hand is an ensemble averaging technique, measuring collective binding events. In this work, SPR was used for characterization of the model surfaces, and to measure binding kinetics of viral glycoproteins to GAGs. The theoretical background of these three techniques will be provided in this chapter. In addition, the concept of fluorescence will be introduced, together with Förster resonance energy transfer (FRET), a method used in this thesis to monitor vesicle fusion.

5.1 Surface plasmon resonance (SPR)

Surface plasmon resonance (SPR) is a widely used technique in biosensing applications. It was introduced in the early 1980s when Liedberg *et al.* demonstrated its potential for gas detection and antibody adsorption[134]. Today SPR is a very popular technique to study protein-ligand interactions, in particular in the context of drug development[135]. It allows the monitoring in real-time of the refractive index change caused by adsorbing molecules to a sensor surface, making it possible to extract information about binding kinetics and affinity of biomolecular interactions.

SPR takes advantage of surface plasmons, which are collective oscillations of free electrons of a metal, arising at the interface between the metal and a dielectric medium when excited by light under certain conditions. The electromagnetic waves coupled to this oscillation are called surface plasmon polaritons. They propagate along the interface and generate an evanescent field on both sides of the interface[136]. The dispersion relation of this two-dimensional waves is given by[137]:

$$k_{sp} = \frac{\omega}{c}\left(\frac{1}{\epsilon} + \frac{1}{\epsilon_m}\right)^{-1/2} \tag{5.1}$$

where ω is the angular frequency, c the speed of light, ϵ_m the real part of the dielectric constant of the metal at the given frequency, and ϵ the dielectric constant of the second medium. Given the nature of the two media, we have $\epsilon_m < 0$, $\epsilon > 0$ and $|\epsilon_m| \gg |\epsilon|$. Equation (5.1) can be simplified to:

$$k_{sp} = \frac{\omega}{c}\sqrt{\epsilon} = \frac{\omega}{c}\, n \tag{5.2}$$

with n being the refractive index of the dielectric medium. If we consider an incident light beam impinging under an angle Θ on the interface, the parallel component of the wave vector is given by:

$$k_x = \frac{\omega}{c}\sqrt{\epsilon}\; sin\Theta \tag{5.3}$$

Excitation of surface plasmons requires phase matching of the wave vectors k_{sp} and k_x[136]. As can be seen from equations (5.2) and (5.3), this is impossible since k_x is always smaller than k_{sp}. To obtain phase matching a different geometry has to be used. If we instead consider a three-layer system, consisting of a thin metal film sandwiched between two insulation media of different dielectric constants ϵ_a and ϵ_g, equations (5.2) and (5.3) become:

$$k_{sp} = \frac{\omega}{c}\sqrt{\epsilon_a} = \frac{\omega}{c}\, n_a \tag{5.4}$$

$$k_x = \frac{\omega}{c}\sqrt{\epsilon_g}\ \sin\Theta = \frac{\omega}{c}\ n_g\ \sin\Theta \tag{5.5}$$

Thus making the solution $k_{sp} = k_x$ possible if $n_g > n_a$.

The most commonly used configuration to achieve surface plasmon excitation in SPR is the Kretschmann configuration[138]. It consists of a glass prism coated with a thin (~ 50 nm) metallic film, usually made of gold (figure 5.1). The light beam hits the interface of the metallic film with an angle higher than the critical angle of total internal reflection (see section about TIRFM for the theory about total internal reflection). When resonance is achieved, the surface plasmons will be excited at the interface between the metal and the ambient medium (usually water). The evanescent field generated by the surface plasmon resonance along the z-axis penetrates the ambient medium by a couple of hundred nanometers, thus making SPR a surface sensitive technique.

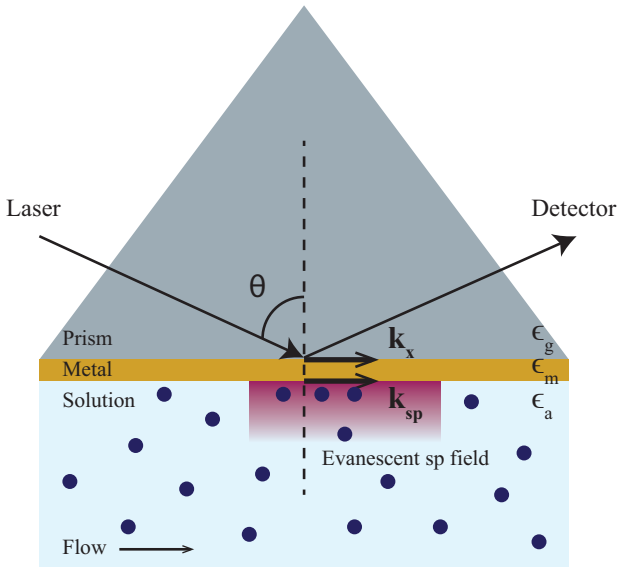

Figure 5.1: *Working principle of SPR using the Kretschmann configuration. A thin metal film coated onto the backside of a glass prism is illuminated with a laser beam in total internal reflection. At a certain angle, surface plasmon resonance is achieved and an evanescent field is created at the metal-solution interface. A change in refractive index upon binding of molecules to the surface will result in a change of resonance angle.*

The main working principle of SPR is that when molecules adsorb to the metal/water interface, the refractive index of the ambient medium n_a will change and resonance will occur at a different angle Θ, according to equations (5.4) and (5.5):

$$k_{sp} = k_x \leftrightarrow \Theta = \arcsin\left(\frac{n_a}{n_g}\right) \tag{5.6}$$

SPR therefore senses small changes in refractive index due to molecular adsorption at the interface causing a shift of the angle at which resonance is obtained. The surface coverage (adsorbed mass per unit area) can be related to the refractive index change Δn, and the difference in resonance angle Δdeg using[139;140]:

$$\Delta\Gamma = \frac{d\Delta n}{(dn/dC)} = \frac{d}{S(dn/dC)[1-\exp(-d/\delta)]}\Delta deg \tag{5.7}$$

In expression (5.7), d is the film thickness, S the sensitivity of the instrument expressed in degrees per refractive index unit, (dn/dC) the refractive index increment per biomolecule concentration in solution and δ the decay length of the intensity of the evanescent field.

5.2 Fluorescence and Förster resonance energy transfer (FRET)

Fluorescence is the emission of light by a molecule, called fluorophore, excited by incident light of a certain wavelength. The fluorophore, initially in the ground energy state S_0, absorbs the energy of the incoming photon to reach the next higher energy state S_1. The energy of the photon must correspond to the energy gap between the two states and typically lies in the visible light spectrum. S_1 being an unstable energy state, the molecule then returns to the ground state via a relaxation process. This relaxation is divided into a vibrational relaxation process and a radiative relaxation process, emitting a photon of lower energy (longer wavelength) than the excitation photon. Figure 5.2 illustrates this process with a Jablonski diagram. The typical lifetime of fluorescence, defined as the average time between excitation and return to the ground state, is around 10 ns[141].

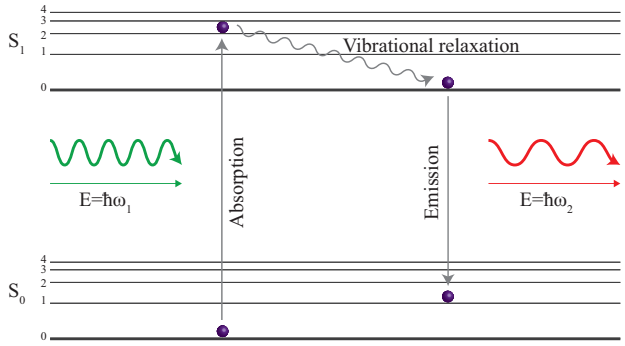

Figure 5.2: *Jablonski diagram illustrating the principle of fluorescence. A fluorophore in the ground state S_0 is excited to the higher energy state S_1 upon absorption of the energy of an incoming photon. During relaxation a photon of longer wavelength (lower energy) is emitted.*

Fluorescence is widely used to image biological samples. The main reason for this is that submicrometer-sized objects interact poorly with ambient light and are therefore hardly

visible in a regular optical microscope. However, thanks to the use of fluorescence, those objects can become visible in a fluorescence microscope. Certain molecules or proteins can be naturally fluorescent (such as the green fluorescent protein (GFP), for example). Alternatively, biomolecules can be fluorescently labeled, by attaching fluorophores via specific functional groups. In this work, we used a membrane-inserting dye to fluorescently label the viral envelope of the HSV particles.

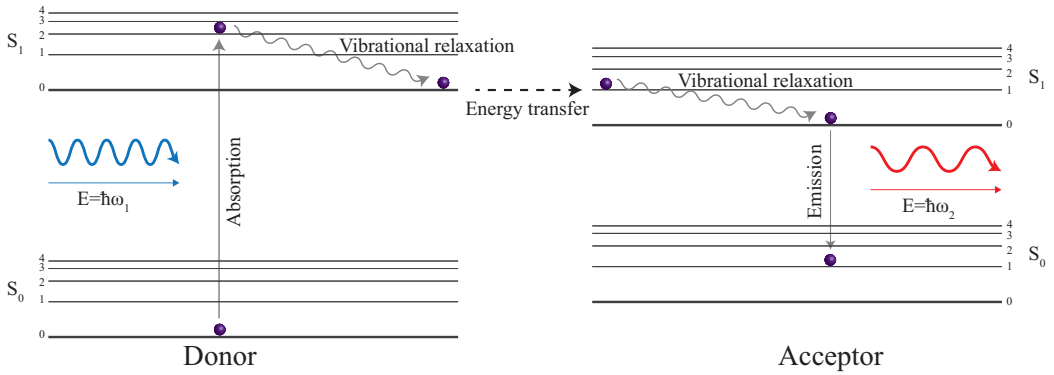

Figure 5.3: *Jablonski diagram illustrating the process of Förster resonance energy transfer (FRET). The energy of the excited fluorophore (donor) is transferred to another fluorophore (acceptor) through a non-radiative process, if the excitation spectrum of the acceptor overlaps with the emission spectrum of the donor. Upon relaxation, the acceptor emits a photon of longer wavelength (lower energy).*

Another possible outcome for a fluorophore in the excited energy state, is an energy transfer via a process called Förster resonance energy transfer (FRET)[142]. FRET occurs when the emission spectrum of one fluorophore (the donor) overlaps with the excitation spectrum of another fluorophore (the acceptor). This process, illustrated in figure 5.3, is a result of a dipole-dipole interaction between the two fluorophores, which makes it a non-radiative energy transfer (there is no intermediate photon). The FRET efficiency E, strongly depends on the intermolecular distance r of donor and acceptor[141]:

$$E = \frac{1}{1 + (r/R_0)^6} \tag{5.8}$$

R_0 is the distance between donor and acceptor at which the energy transfer is 50%, also called Förster distance, given (in Å) by[141]:

$$R_0 = 9.78 \times 10^3 \sqrt[6]{\frac{\kappa^2 Q_D}{n^4} J(\lambda)} \tag{5.9}$$

where κ^2 describes the relative orientation between the dipoles of donor and acceptor, Q_D is the quantum yield (number of emitted photons over number of absorbed photons), n is the refractive index of the medium, and $J(\lambda)$ describes the spectral overlap between donor

emission and acceptor excitation (in $M^{-1}cm^3$). R_0 is typically in the range of 30 to 60 Å[141]. Because of the strong dependency of the FRET efficiency on the distance between the two fluorophores, FRET serves as a useful method to estimate intermolecular distances in the nanometer range. For example, FRET assays have been used to detect biomolecular interactions, such as protein-protein interactions[143], to study protein folding[144], and to monitor vesicle fusion[145]. In **paper V**, we used a FRET assay to estimate the mixing efficiency of synthetic vesicles with native membrane vesicles, as well as to quantify these native membrane vesicle suspensions.

5.3 Total internal reflection fluorescence microscopy (TIRFM)

Total internal reflection fluorescence microscopy (TIRFM) is a technique combining three key elements: microscopy, fluorescence and total internal reflection. All of these elements had been widely used independently before Daniel Axelrod combined them to image cell structures in contact with a solid substrate in the early 1980s[146]. The full theory behind the technique was described three years later[147]. Since then, TIRFM has been used for a wide range of applications, many of them of biological nature.

TIRFM is primarily a fluorescence microscopy technique. It takes advantage of the discrepancy between fluorescence excitation and emission wavelengths (see figure 5.2) to simultaneously activate and detect the signal of fluorescent probes. A common TIRFM setup (figure 5.5) uses a white light source in combination with an excitation filter, selecting a range of wavelengths that overlaps with the excitation spectrum of the fluorophore in the sample, and an emission filter, to allow only light originating from the fluorescent probe to reach the camera. Alternatively, laser setups can be used instead of the white light source to illuminate the sample.

The element that distinguishes TIRFM from regular fluorescence microscopy is the total internal reflection (TIR) setup. To explain the principle of TIR one uses geometrical optics. Snell's law describes how a light beam behaves when impinging on an interface of two media with different refractive indexes n_1 and n_2:

$$n_1 \sin \Theta_1 = n_2 \sin \Theta_2 \tag{5.10}$$

Θ_1 and Θ_2 are the angle of incidence and angle of refraction, respectively. This formula shows how the angle of refraction depends on the angle of incidence and the refractive indexes of the two media. If the second medium is of lower refractive index ($n_2 < n_1$), the refracted beam will travel along the interface of the two media at $\Theta_1 = \Theta_c$. This angle, called critical angle, is given by:

$$\Theta_c = \arcsin\left(\frac{n_2}{n_1}\right) \tag{5.11}$$

For angles equal to or greater than the critical angle ($\Theta_1 \geq \Theta_c$) the incident beam is totally reflected at the interface. This situation is called total internal reflection and represented schematically in figure 5.4.

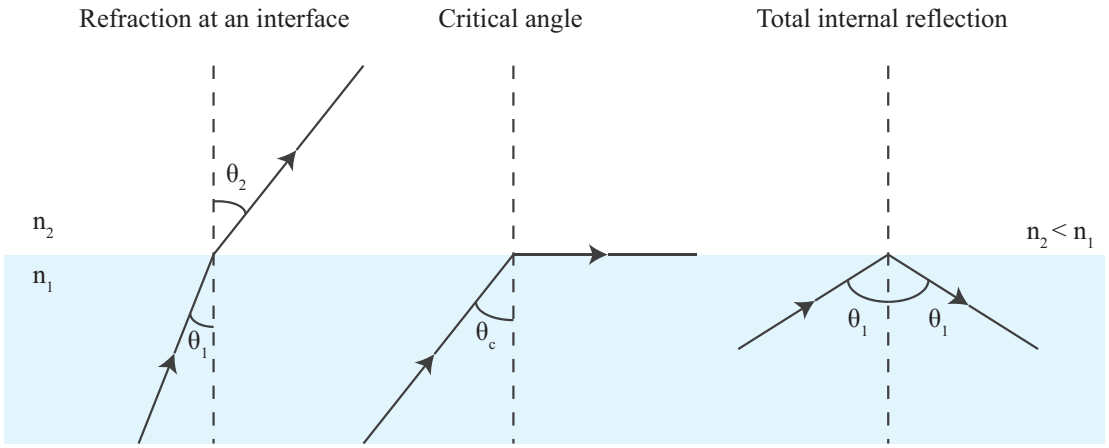

Figure 5.4: *Illustration of Snell's law and the principle of total internal reflection. For incident angles equal to or greater than a critical angle Θ_c, the incident beam is totally reflected at the interface with a lower refractive index medium.*

An evanescent field is then created at the interface, extending a small distance into the optically thinner medium. The intensity I of this evanescent field at a distance z from the interface is given by[148]:

$$I(z) = I_0 \; exp\left(\frac{-z}{d}\right) \tag{5.12}$$

I_0 is the intensity at the interface and the characteristic exponential decay depth d is defined as:

$$d = \frac{\lambda}{4\pi n_2}\left(\frac{\sin^2\Theta_1}{\sin^2\Theta_c} - 1\right)^{-1/2} \tag{5.13}$$

with λ denoting the wavelength of the incident light.

The exponential decay depth d is usually on the order of the wavelength λ or smaller, meaning that only fluorescent molecules within a couple of hundred nanometers away from the surface will be excited by the incident light, while particles in the bulk solution remain invisible. This principle makes TIRFM a surface sensitive technique, well-suited to be used in combination with surface-based assays, like the ones presented in chapter 4.

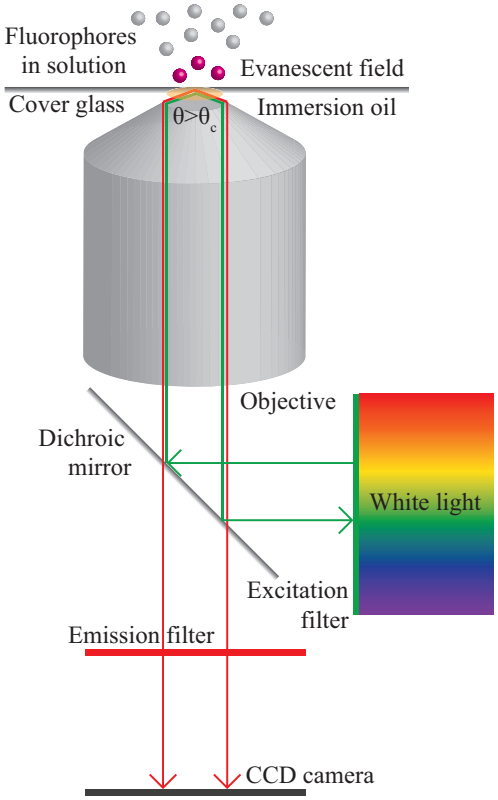

Figure 5.5: *Working principle of TIRFM including the three main key elements: fluorescence, optical microscopy and total internal reflection. An excitation filter selects an appropriate range of wavelengths from a white light source to excite the fluorescent probes. A dichroic mirror is used to direct the light to the objective, whose crescent-shaped aperture generates total internal reflection of the incident light. The fluorescent light emitted from the sample passes an emission filter (that sorts out the excitation light) and is collected by a camera.*

5.4 Atomic force microscopy (AFM)

The atomic force microscope (AFM) was invented by Gerd Binnig, who patented the technique and, together with Calvin F. Quate and Christoph Gerber, published its first experimental implementation[149] in 1986. Binnig was also one of the inventors of the precursor technique, the scanning tunneling microscope (STM), for which he was awarded the Nobel Prize in Physics in 1986, together with Heinrich Rohrer[150]. Both techniques were developed to image surfaces with atomic resolution by scanning the sample with a mechanical probe, which is brought into very close proximity to the surface. In STM a voltage is applied between the conducting probe and the sample, leading to a transfer of electrons, called tunneling current. During an x-y scan, the probe is moved across the sample to measure the tunneling current for each position and determine, amongst others, the topography of the surface. While STM relies on the conductive properties of the sample, an AFM directly measures the force exerted by the surface onto the probe and can therefore

be applied to the study of both conductors and insulators. Thanks to the possibility of using the instrument in different media such as vacuum, air, but also liquid environments, AFM has, since its first commercial appearance in 1989, been used for a wide range of applications. One field of application that has considerably increased in popularity in the past decade is cell biology and microbiology, as the AFM has proven itself to be a powerful tool for probing biological samples, such as living cells and bacteria[151;152], proteins[153–155], viruses[156–158], and DNA[159;160].

The basic working principle of a typical AFM instrument is shown in figure 5.6. The scanning probe, usually denoted AFM tip, is attached to a spring-like cantilever. When the tip is approached to the surface the force emerging between surface and tip will cause a deflection of the cantilever's free end. This deflection distance is usually measured using an optical system, consisting of a laser beam that is reflected on the apex of the cantilever and whose signal is collected by a photodiode. To perform a scan of the surface, either the cantilever or the sample is coupled to a piezoelectric element, which deforms when exposed to a voltage, thereby allowing very small and accurate displacements.

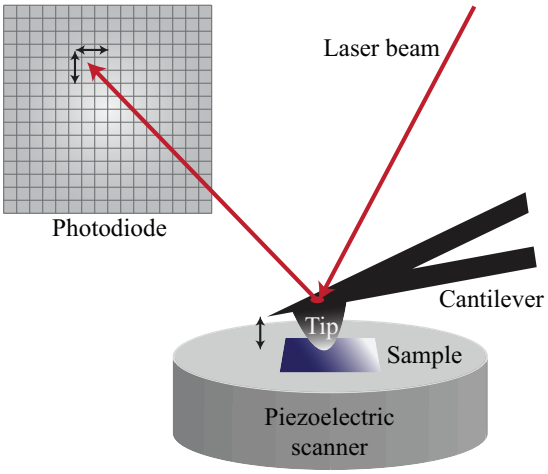

Figure 5.6: *Schematic representation of a typical AFM. A probe, usually called AFM tip, is attached to a cantilever and approached to the sample surface. The deflection of the cantilever upon interaction between tip and surface is measured using an optical readout system consisting of a laser beam and a photodiode. To perform a scan of the sample surface, a piezoelectric scanner is used.*

Since its introduction, the AFM has become a well-established tool for topographic imaging. But besides imaging, the AFM is also increasingly used for force spectroscopy, due to its ability to directly measure the tip-sample interactions and to generate force-distance (*FD*) curves[161]. This, together with the possibility of functionalizing the AFM tip with biomolecules of interest[162], has opened up the way for *FD*-based AFM to become a valuable tool to study ligand-receptor interactions[153;163–165]. Typically, the molecule of interest is attached to the AFM tip via a polymeric linker and the cantilever performs sequential approach and retraction cycles (figure 5.7a), during which the cantilever deflection is mon-

itored. From the measured cantilever deflection δ_c, one can calculate the force F, using Hooke's law[161]:

$$F = -\kappa_s \, \delta_c \tag{5.14}$$

The constant κ_s denotes the effective spring constant of the system, determined by the spring constant of the cantilever and the elastic constants describing the tip functionalization complex and the sample deformation. The measured force can be expressed in terms of tip-sample distance $D = z - \delta_c$, with z denoting the controlled distance, *i.e.* the distance at rest between cantilever and surface:

$$F(D) = -\kappa_s \, (z - D) \tag{5.15}$$

Equation (5.15) shows the relation between measured force and tip-sample distance, which is represented in the *FD* curve (figure 5.7b). One usually draws both the approach and retraction curve, from which one can extract information about, for example, the sample thickness, deformation, and elasticity. From the retraction curve one also extracts the adhesion force that, upon contact, emerges between the ligand on the functionalized AFM tip and the receptor molecule in the sample.

As predicted by the Bell-Evans theory[166–169], the measured bond rupture force of the ligand-receptor pair depends on the applied loading rate (r_f) in N/s, which is defined as[168]:

$$r_f = \kappa_s v_{pull} \tag{5.16}$$

where v_{pull} is the pulling velocity (derivative of the tip oscillation[170]). In a typical force spectroscopy experiment, r_f is not constant, as the applied force is usually increased until bond rupture is achieved. r_f can then be calculated from the slope of the force-time curve directly prior to the bond rupture event[170] (figure 5.7a).

To conceptualize the dependence of measured adhesion force on loading rate, it is useful to visualize the free energy landscape of a bond (figure 5.7c), which, in particular for weak noncovalent bonds governing biomolecular interactions, is fully explored by thermal fluctuations[167]. In this free energy landscape, the bond is represented as a local minimum energy state, characterized by a sharp energy barrier E_b that needs to be overcome to break the bond. The likelihood of reaching the transition state (*i.e.* bond breakage) is given by the dissociation rate constant:

$$k_{off} \sim \exp\left(\frac{-E_b}{k_B T}\right) \tag{5.17}$$

which also determines the lifetime of the bond:

$$t_{off} = \frac{1}{k_{off}} \tag{5.18}$$

When applying an external pulling force (F_L) to the system, the time of survival of the bond is decreased, which can be represented by a lowering of the energy barrier E_b in the energy landscape[169]. As a consequence, the off rate of the bond is increased by a factor $\exp(-F_L/F_\beta)$, where

$$F_\beta = \frac{k_B T}{x_\beta} \tag{5.19}$$

x_β represents the reaction coordinate at the transition state. Thus, if a fast loading rate is applied (high applied force over time), the bond will have a short lifetime, but withstand large forces, since the likelihood of stochastic bond rupture through thermal activation is low. From the Bell-Evans theory it follows that the most frequently observed rupture force F^* shows a linear behavior when plotted against the logarithm of the applied loading rate r_f (figure 5.7d). This relationship is written as follows[169]:

$$F^* = F_\beta \; log_e \left(\frac{r_f}{k_{off} F_\beta} \right) \tag{5.20}$$

Equation (5.20) can be used to extract the dissociation rate constant k_{off} for the studied bond, as well as the reaction coordinate x_β. In case of multiple bonds, the energy landscape can become more complex, *e.g.* showing a cascade of energy barriers, each characterized by their individual energy barrier height E_b and width x_β. Plotting rupture force F^* against the logarithm of the applied loading rate r_f will give rise to multiple linear regimes, corresponding to the individual bonds[167], from which one can extract k_{off} and x_β values for each bond.

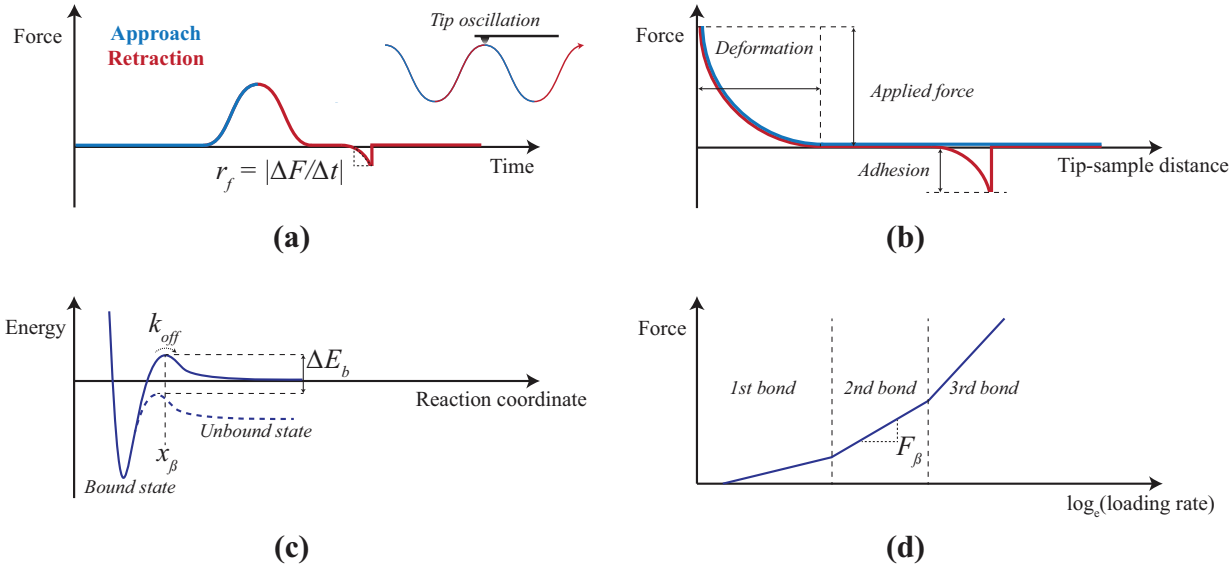

Figure 5.7: *Force-distance based AFM.* ***(a)*** *The cantilever is oscillated at a set frequency, performing cycles of approach and retraction. From the cantilever deflection, one calculates the force F using Hooke's law. The force-time curve is used to extract the loading rates (r_f; slope of the curve directly prior to the bond rupture event)* ***(b)*** *Force-distance curves are used to determine the adhesion force between the functionalized tip and the surface.* ***(c)*** *Applying a mechanical pulling force to the system changes the energy landscape of the bond towards lower dissociation energy barriers.* ***(d)*** *The force follows a linear relationship with regards to the logarithm of the loading rate. The slope of the linear curve is given by $F_\beta = \frac{k_B T}{x_\beta}$, where x_β represents the reaction coordinate at the transition state. For multiband reactions, different linear regimes will appear.*

6

Results

"Research is formalized curiosity. It is poking and prying with a purpose."
– Zora Neale Hurston

This thesis focuses on the interactions between HSV and the cell membrane during initial attachment and release. Using traditional cell-based assays, the main actors of these processes have been identified to be viral glycoproteins gC and gB, and cell-surface GAGs. In order to gain further insights into the dynamic mechanisms regulating attachment and release, and to probe HSV-cell membrane interactions on a molecular level, our strategy was to complement cell-based assays with bioanalytical model platforms, designed to mimic the architecture of the native cell membrane. The advantage of such model platforms is twofold: First, they allow us to isolate the interactions occurring at the membrane from other cellular processes; second, they are compatible with surface-based sensing methods, allowing for high sensitivity interaction studies, down to the single particle level, which is an advantage, for example, when working with samples of high heterogeneity.

Two cell membrane mimics were implemented in this work. The first one was based on end-grafted GAG chains, allowing us to focus solely on the HSV-GAG interactions. The second one was derived from native cell membranes, to include the whole milieu of cell membrane receptors, and probe HSV binding characteristics in a more native-like environment. These model platforms, introduced in the first section of this chapter, were used in combination with SPR, TIRFM, and *FD*-based AFM to measure binding kinetics, particle mobility, and binding forces. Two factors likely to influence the characteristics of the HSV-cell membrane interactions were investigated. The first one was the physicochemical properties of the GAGs, discussed in **paper I**. **Paper II-IV** focus on the role of the viral glycoproteins, and in particular their glycosylation, in regulating attachment and release of HSV-1 (**paper II** & **III**) and HSV-2 (**paper IV**).

This chapter provides a summary of the main aims and findings of the appended papers. For an in-depth discussion of the results, and experimental details, the reader is referred to the respective paper.

6.1 Bioanalytical platforms to probe HSV-cell membrane interactions

Because of their essential role during initial HSV attachment, the HSV-GAG interactions are the main focus of this work. To be able to study these interactions in a controlled way, we implemented a platform (herein called GAG platform), which mimics the presentation of GAGs in the extracellular matrix and at the cell surface. The GAG chains were end-grafted to a sensor surface, thereby creating a brush-like architecture, which resembles the natural attachment of GAGs to proteoglycans. The platform is based on a planar SLB (or self-assembled monolayer in **paper II**), providing surface passivation, and a support to attach the GAG chains using biotin/streptavidin coupling[171;172] (illustrated in figure 6.1a). The surface functionalization was monitored in real-time using surface plasmon resonance (SPR) to determine the surface densities of the end-grafted GAGs (**paper I**).

The GAGs used in this work were chondroitin sulfate (CS), heparan sulfate (HS), hyaluronic acid (HA), and sulfated hyaluronic acid (sHA). CS and HS are native GAGs, known to interact with HSV-1 and HSV-2[7;46]. These molecules are sulfated through enzymatic action, which confers a high degree of heterogeneity to their sulfation patterns. In contrast, sHA originates from chemically sulfated HA chains, and therefore most likely presents a more homogeneous distribution of sulfate groups. sHA was used, for example, in **paper I** to study the importance of the native arrangement of sulfate groups along the GAG chain. HA is the only GAG that is not sulfated and was therefore used as a negative control to test the specificity of HSV binding to sulfated GAGs.

The GAG platform was used in **paper I - IV**, in combination with SPR, to measure binding kinetics of purified gC glycoproteins to GAGs (CS and sHA), TIRFM to measure binding kinetics and lateral diffusion of entire HSV virions, and *FD*-based AFM to measure binding forces of the HSV-GAG interaction.

To complement our GAG platform, we were interested in a second platform, of higher compositional complexity, to create a more native-like interaction environment that includes all cellular membrane receptors. We opted for a top down approach, namely nSLBs derived from native cell membrane material (introduced in chapter 4), which offer high compositional complexity, compatible with surface-based methods (figure 6.1b). In particular, we chose to implement a method to create nSLBs from native cell membrane material, which had recently been developed in our laboratory[118]. This method is based on mechanical disruption of cell membranes to obtain native membrane vesicles (NMVs), which are sonicated with synthetic vesicles to facilitate vesicle rupture into planar SLBs.

This newly developed nSLB platform was used for the first time to probe virus-cell membrane interactions in **paper V**. The aim of this paper was to assess the potential of nSLBs to be used in combination with TIRFM to study HSV-1 binding kinetics and mobility. To this end, we chose a series of applications aimed at demonstrating the possibility of using nSLBs for both fundamental interaction studies, as well as for screening of antiviral

inhibitors. We altered both the expression of viral glycoproteins (using mutant HSV-1 variants deficient in gC glycoproteins) and the composition of the nSLBs (through enzymatic removal of HS). For both cases, this led to significant reductions in apparent HSV-1 binding affinities. Furthermore we used heparin as a model antiviral compound[173], for which we could estimate the IC_{50} value, providing a measure of its inhibition efficiency.

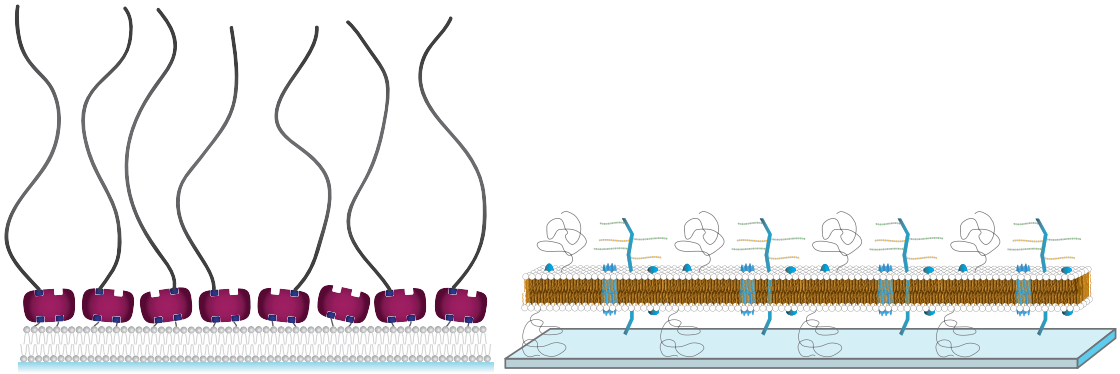

Figure 6.1: ***(a)*** *The GAG platform (used in* ***paper I - IV****) mimics the attachment of GAGs to proteoglycans in the extracellular matrix and on the cell surface.* ***(b)*** *The nSLB platform used in* ***paper V*** *is derived from native membrane vesicles, obtained from mechanically disrupted cells, which are incorporated into planar SLBs. (Illustration by Eneas Schmidt)*

6.2 Influence of the sulfation of glycosaminoglycans

The main research question addressed in **paper I** was how the physicochemical properties of GAGs, in particular the nature of their sulfation, influence the binding characteristics of HSV-1. Our hypothesis was that besides the number of sulfate groups, their specific arrangement along the GAG chain could play a significant role during HSV binding. To verify this hypothesis, we probed binding of single fluorescently labeled HSV-1 particles to native CS and HS, as well as artificially sulfated sHA, using TIRFM (figure 6.2a). The recorded time-lapse movies were analyzed using both single particle tracking (SPT), to study the diffusive behavior of GAG-bound HSV-1 particles, and equilibrium fluctuation analysis (EFA), to quantify HSV-1 binding kinetics (see chapter 3 for the formalism of SPT and EFA).

The SPT studies (figure 6.2b,c) revealed complex diffusion characteristics of GAG-bound HSV-1 particles, presenting both normal and anomalous diffusion modes. While no clear trend could be resolved for the normal diffusion mode, anomalously diffusing particles, which also exhibited the fastest diffusion (with diffusion coefficients of up to 0.1 $\mu m^2/s$), showed significantly faster diffusion on native CS and HS as compared to sHA. This increased mobility on native GAGs could not be explained by differences in chain or sulfate

group densities. Indeed, the fastest diffusion was obtained on HS, which also yielded the highest chain and sulfate group density, although diffusion coefficients are expected to decrease with the number of bonds[174]. Our findings therefore suggest that the type of GAG influences HSV mobility, which could be a consequence of both the number and arrangement of sulfate groups along the GAG chains.

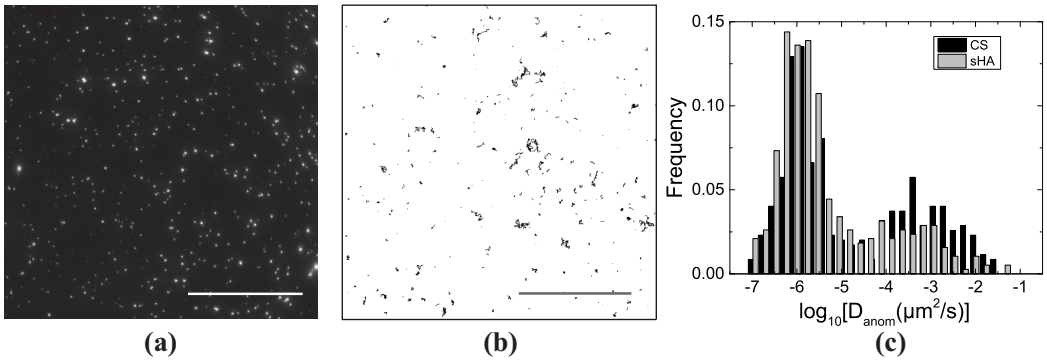

Figure 6.2: *In **paper I** we studied among others the diffusive behavior of GAG-bound HSV-1 virions. **(a)** TIRFM image showing fluorescently labeled HSV-1 particles bound to a CS-coated surface. Scale bar:* 50 μm. *__(b)__ Trajectories of the particles in (a) obtained from SPT analysis. Scale bar:* 50 μm. *__(c)__ Histogram of diffusion coefficients from anomalously diffusing HSV-1 particles on CS and sHA.*

Association rates, determined by EFA, were in a similar range for CS, HS, and sHA, with somewhat more particles binding to CS. In comparison, non-sulfated HA yielded 10 times lower binding, demonstrating the specificity of the HSV-1 interaction to sulfated GAGs. In an attempt to qualitatively compare binding rates, we calculated association rates per GAG, which revealed highest binding propensities for CS ($\sim$ 3 times higher in comparison to sHA), although this GAG had the lowest amount of sulfates per molecule. This result supports the above stated hypothesis that not only the degree of sulfation of the GAG chain, but also its type of sulfation influences the affinity of the HSV interaction. Analysis of the dissociation of particles revealed that only very few particles leave the surface (less than 0.5% of the bound HSV particles dissociated from the GAG surfaces), highlighting the efficiency of GAGs in recruiting viruses to the cell surface.

Taken together, **paper I** demonstrates that both the lateral diffusion and the binding kinetics of GAG-bound HSV-1 particles are influenced by the type of GAG, suggesting that the arrangement of sulfate groups on native GAG chains could play a role in promoting and modulating HSV binding. Based on our observations, we propose that GAG-bound HSV particles perform a stochastic "wobbling" movement originating from a gradual exchange of bonds between the virus and the GAGs, which does not rely on receptor mobility, analogous to the recently suggested mechanism of influenza virus A[128]. Although still hypothetical at this point, this lateral diffusion via bond exchange could play an important role during HSV cell infection, to allow the virus to travel through the extracellular matrix

and along the cell surface in search for suitable entry sites. As a first step towards confirming this hypothesis, we performed SPT analysis on HSV-1 particles bound to nSLBs, to characterize their mobility in a more native-like environment, which includes all membrane components. A similar diffusive behavior was observed in this case (**paper V**), with the main difference that all mobile virions were found to undergo anomalous diffusion. While it is at this point not clear where this difference stems from, one reason could be that the contribution to the measured HSV diffusion from mobile surface receptors (often of anomalous nature[175]) is expected to be considerably higher for the nSLB system. The next step towards demonstrating the biological significance of the observed wobbling movement is to perform live-cell SPT studies, as further discussed in chapter 7.

6.3 Role of the glycosylation of viral glycoproteins

Paper II - IV address the role of the glycosylation of the viral glycoproteins in modulating HSV attachment and release to/from the cell surface. In particular, we discuss the function of so-called mucin-like regions, which have been found, for example, on glycoproteins gC-1 (on HSV-1) and gG-2 (on HSV-2), forming extended structures of numerous clustered *O*-linked glycans. Such highly glycosylated regions have been suggested to protect viruses from unwanted interactions, for example with neutralizing antibodies[57;58]. The motivation behind **paper II - IV** was that the mucin-like regions on gC-1 and gG-2 could play an essential role in balancing the HSV-GAG interaction. This hypothesis was based on experiments showing that these domains are affected by serial passages of HSV in cultured cells in the presence of the GAG mimetic muparfostat (PI-88), inhibitor of HSV binding. Indeed, for both HSV-1 and HSV-2, several passages resulted in the selection of viral mutants, which were deficient in the mucin-like domains. In the case of HSV-1 mutants the gC-1 glycoproteins were truncated, lacking their mucin-like domain[176], while the HSV-2 mutants were missing the entire gG-2 glycoproteins[177]. These observations suggested that the presence of mucin-like complexes on viral glycoproteins might influence the HSV-GAG interaction characteristics. To confirm this hypothesis we used cell-based studies in combination with the GAG platform, to study HSV binding and release both in their natural cell environment, and on GAGs only. The case of HSV-1 was studied in **paper II** and **paper III**, while **paper IV** was dedicated to HSV-2.

6.3.1 HSV-1

The aim of **paper II** was to investigate the role of the mucin-like domain on gC-1. Our strategy was to employ HSV-1 variants lacking the entire mucin-like region on the gC glycoproteins (KOSc-gCΔmuc), as well as their corresponding purified gC glycoproteins (gCΔmuc). Electron microscopy studies on infected cells revealed that the number of spontaneously released KOSc-gCΔmuc virions from the surface of infected cells was more

than 20 times lower than for the wild-type strain. Furthermore, SPR binding studies of purified gCΔmuc glycoproteins to surface-grafted sHA and CS chains (using the GAG platform as described above) showed that gCΔmuc had less of a propensity to bind to GAGs in comparison to wild-type gC, but that once bound, the gCΔmuc-GAG complex was more stable. In addition, we studied the association of KOSc-gCΔmuc to CS using TIRFM and compared the results to the association of wild-type HSV-1 (KOSc WT) (figure 6.3a). In agreement with our observations on purified glycoproteins, mutant HSV-1 particles associated to a lesser extent to the GAG surface in comparison to the wild-type virus ($\sim$ 15% of the KOSc WT association). These findings confirmed our hypothesis that the mucin-like region on gC-1 modulates the attachment and release of HSV-1 to GAGs.

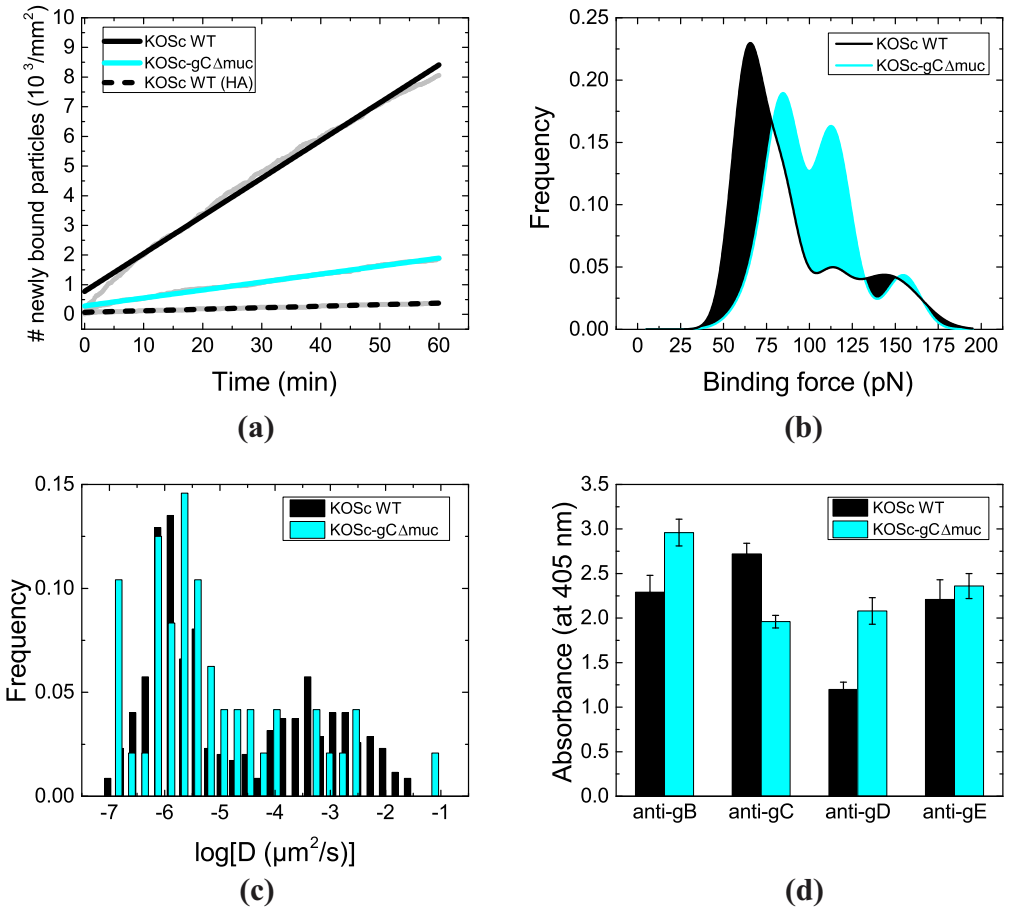

Figure 6.3: *Investigating the role of the mucin-like region on gC-1 using* ***(a)*** *TIRFM in combination with equilibrium fluctuation analysis to measure association kinetics,* ***(b)*** *FD-based AFM to measure binding forces,* ***(c)*** *TIRFM in combination with SPT to quantify mobility, and* ***(d)*** *an ELISA-based assay to measure the accessibility of different glycoproteins, for both the wild-type (KOSc WT) and mutant (KOSc-gCΔmuc) HSV-1 virus.*

To further elucidate the role of the mucin-like region on glycoprotein gC of HSV-1, we investigated how its presence influences the binding forces and diffusive behavior of HSV-1 interacting with CS. These studies, presented in **paper III**, were performed using *FD*-based AFM, and TIRFM in combination with SPT. The AFM results revealed that the binding forces (representing the force needed to disrupt the virus-GAG interaction) were overall higher for HSV-1 in the absence of the mucin-like domain on gC (figure 6.3b). In addition, our SPT studies showed decreased mobility for the HSV-1 mutants (KOSc-gCΔmuc) in comparison to the wild-type (figure 6.3c). These findings are in line with the results in **paper II**, demonstrating that the deletion of the mucin-like domain induces a direct change in binding kinetics of gCΔmuc with CS, notably by impairing its ability to dissociate. This change is expected to affect the overall binding strength of HSV-1 to CS, as well as the ability of the virus to disrupt and reform single bonds, necessary for its lateral diffusion. Besides affecting gC, the deletion of the mucin-like region could also alter the contribution to the overall interaction from other glycoproteins, such as gB and gD. To verify this hypothesis we performed an ELISA-based antibody assay to test the accessibility of envelope glycoproteins gB, gC, gD, and gE, both in the presence and in the absence of the mucin-like domain. As shown in figure 6.3d, we observed that the accessibility of the GAG binding site on gC was reduced on KOSc-gCΔmuc as compared to KOSc WT, while gB and gD showed enhanced accessibility in the absence of the mucin-like region. The accessibility of gE, which we used as a control, appeared unchanged. These findings suggest that the mucin-like region on gC promotes GAG interactions via gC, while shielding possible binding sites on gB and gD. Therefore, it is likely that the deletion of the mucin-like domain could induce a preferential involvement of gB and gD to the overall HSV-GAG interaction, which could lead to an increased number of glycoprotein-CS bonds, contributing to the observed stronger binding and reduced mobility of KOSc-gCΔmuc. Taken together, based on the findings in **paper II** & **III**, we postulate that one role of the mucin-like region on gC is to regulate the attachment of HSV-1 to GAGs by enhancing initial binding via gC, and preventing premature involvement of gB and gD, likely to result in trapping of the virus on the cell surface during initial attachment or final egress.

6.3.2 HSV-2

Paper IV was entirely dedicated to HSV-2. The aim was to investigate the role of its mucin-like glycoprotein gG-2, which was formerly not known to be involved in virus attachment to GAGs. To this end, we performed both cell infection studies, and TIRFM experiments (using the GAG platform), for which we employed a wild-type HSV-2 virus, as well as a mutant variant, which completely lacked the gG glycoproteins.

Cell infection experiments showed that gG-deficient HSV-2 mutants were able to infect cells but yielded ~ 200 times fewer virus particles in the cell culture medium in comparison to the HSV-2 wild-type, which was a consequence of the mutants getting trapped on the surface of infected cells. To complement these findings we used TIRFM in combination

with EFA and SPT to study binding kinetics and mobility of mutant HSV-2 particles bound to end-grafted CS chains. While particle dissociation was generally low (less than $\sim 3\%$ for both virus strains), as already observed for HSV-1 particles in **paper I**, association rates were found to be on average ~ 4.5 times higher for the gG-deficient HSV-2 variants in comparison to the wild-type (figure 6.4a). Furthermore, the mutant virus exhibited decreased mobility in comparison to the wild-type (figure 6.3b). These findings indicate that the mucin-like glycoprotein gG balances the virus interaction with GAGs to prevent formation of non-reversible bonds leading to trapping of the virus on the cell surface. While it remains unclear how exactly gG executes this role, we performed antibody binding tests which showed a reduced accessibility to the binding proteins gC-2 and gB-2 in the presence of gG. This interesting observation promoted the idea that gG could selectively shield GAG binding sites on HSV-2 to ensure reversibility of the HSV-GAG interaction, and prevent trapping.

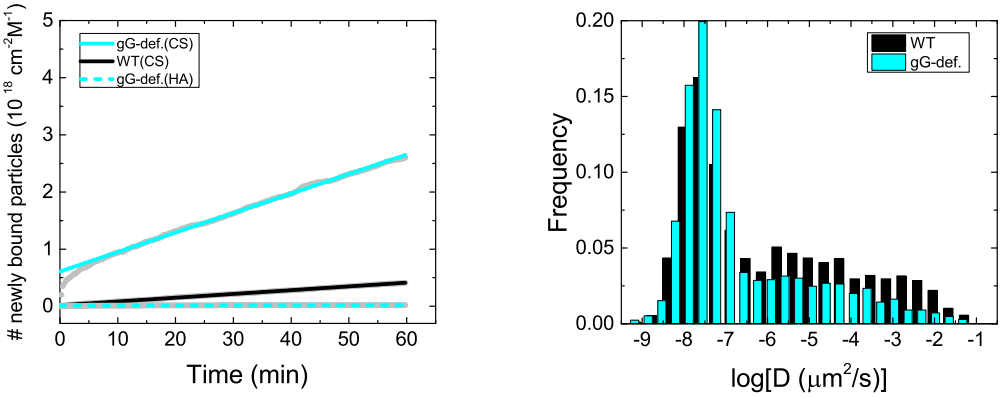

Figure 6.4: ***Paper IV*** *focused on studying the role of the mucin-like gG-2 glycoprotein (on HSV-2).* ***(a)*** *Association kinetics of wild-type (WT) and mutant (gG-def.) HSV-2 virions to CS-coated surfaces.* ***(b)*** *Histogram of diffusion coefficients (normal and anomalous diffusion combined) of the CS-bound HSV-2 virions.*

6.3.3 Concluding remarks

Taken together, the results presented in **paper II - IV** demonstrate that both HSV-1 and HSV-2 take advantage of the glycosylation of their glycoproteins to balance the interaction of the virus with cell-surface GAGs during initial attachment and egress. Although the location of the mucin-like domains differed between the two serotypes, we found that in both cases their deletion led to trapping of viral particles on the surface of infected cells, and a reduced mobility on GAGs. Furthermore, the mucin-like domains were found to shield other glycoproteins (gB and gD for HSV-1; gB and gC for HSV-2), likely to limit their

contribution to GAG binding. Our findings suggest that these highly glycosylated domains could have one common function, which is to prevent trapping of virions upon initial cell attachment and release. Mucin-like domains form extended structures, frequently containing negatively charged sialic acid residues, which by steric hindrance and electrostatic repulsion with the negatively charged sulfate groups on the GAG chains could contribute to the reversibility of the HSV-GAG interaction. While our studies only focused on HSV, similar mucin-like structures have been found on a number of other viruses, including the Ebola virus, HIV, and the respiratory syncytial virus[57]. It is therefore possible that more viruses, especially other GAG-binding viruses, use similar mechanisms to promote virus mobility on the cell surface, and ensure successful liberation of progeny virus after infection.

7

Final reflections and outlook

"Sometimes questions are more important than answers." – Nancy Willard

The work presented in this thesis is the result of multiple projects and collaborations, all grouped under one main research aim: to understand the molecular mechanisms of HSV attachment and release to/from the cell surface. Our strategy was to complement traditional cell-based assays with bioanalytical platforms, designed to mimic the cell membrane, in order to characterize HSV-cell membrane interactions on a molecular level. The first platform, the GAG platform, was a purely artificial model, mimicking the brush-like architecture of GAGs close to the cell surface. It provided us with the means of characterizing HSV-GAG interactions in a controlled manner, with the possibility of altering distinct physicochemical properties of the GAG chains. The second platform was derived directly from the native cell membrane, thereby creating an interaction environment closer to the natural cell environment. Both platforms were used mainly in combination with TIRFM, to study binding kinetics and particle mobility, in order to demonstrate the role of specific viral and cellular components during cell surface attachment and release.

In this final chapter, two aspects discussed in this thesis will be developed further. The first one is the use of nSLB systems for virus interaction studies. **Paper V** demonstrated the potential of nSLBs to be used both for fundamental virus interaction studies, as well as for screening of antiviral compounds. For example, the principal involvement of glycoprotein gC-1 and cellular HS during initial HSV attachment was well established prior to our study, thanks to traditional cell-based assays, but could be confirmed and quantified using our native-like model systems. These promising results highlight the potential of nSLBs to be used in the future to identify the main molecular actors involved in cell attachment for poorly studied viruses, and new emerging virus strains. Such knowledge is essential to the development of new antiviral therapies, targeting binding sites on either the virus or the cell surface to prevent virus attachment. To test such inhibitor compounds, nSLBs can be used as screening platforms, as confirmed by our inhibition test using heparin. The high versatility of nSLBs, which can in principle be adapted to any cell line and virus type, will

hopefully promote their use in the future.

A second aspect, which deserves a more in-depth discussion, is virus mobility, a central theme in this thesis. Single particle tracking was not initially planned to be part of this thesis work, but was included when the early TIRFM movies of HSV-1 binding to GAG-coated surfaces showed clear signs of lateral diffusion. Our observations led us to propose that HSV virions, multivalently attached to the GAG chains, undergo a wobbling movement, caused by the disruption and reformation of single bonds. Although the diffusive behavior of HSV particles was characterized on model membranes, and is therefore most likely not fully representative of HSV mobility on live cell membranes, this wobbling movement could play a significant role during cell infection. Virus binding to the cell membrane is often described as a two-step interaction[178]: primary attachment, mediated by weak interactions between viral proteins and cellular attachment factors (for example electrostatic binding to GAGs), followed by secondary, non-reversible binding to specific membrane receptors facilitating cell entry. In the past decade, there has been an increasing number of reports aiming to elucidate the dynamic processes occurring between primary and secondary attachment. The main question motivating this research is how viruses reach membrane regions of high receptor densities, which they rely on to become internalized by the cell. Different possible pathways have been suggested[178], from which one, the *land and seek* approach (figure 7.1), postulates that viruses diffuse along the cell membrane immediately after landing, either as a virus/receptor complex, or alone via disruption and reformation of bonds, in search for suitable entry sites. Similar mechanisms have been reported for a number of viruses[68;124–130].

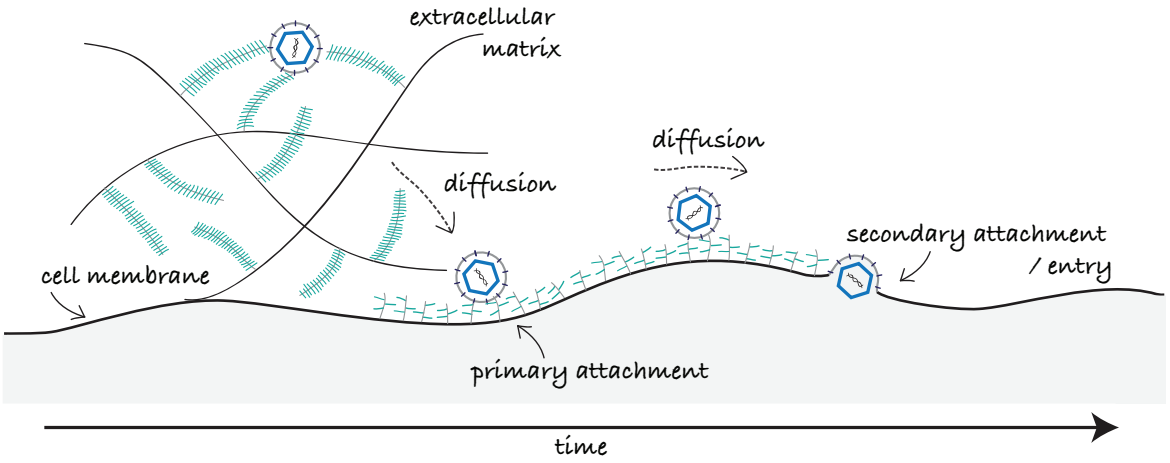

Figure 7.1: *Illustration of the land and seek approach, postulating that viruses can diffuse along the cell membrane immediately after landing in search for suitable entry sites. Based on the findings of this thesis, we propose that this diffusion could already start in the extracellular matrix, where gradients of GAG sulfation could guide the virus towards the cell membrane. Mucin-like domains on the glycoproteins could play an important role during this process to balance the interactions with GAGs, and prevent premature trapping.*

While our strategy throughout this thesis was to use model surfaces to confirm and elucidate results previously obtained from cell-based assays, the reverse approach is needed in this case. Indeed, to confirm the biological significance of the virus mobility, initially observed on our cell membrane mimics, it is imperative to move towards cell-based systems, and perform live-cell SPT studies to monitor the early steps of HSV cell infection. **Paper I** suggests that the sulfation of the GAG molecules plays an important role in modulating diffusion at the cell surface. Therefore one could hypothesize that GAGs play a crucial role in mediating virus diffusion already in the extracellular matrix, rich in GAGs such as chondroitin sulfate, where gradients of GAG sulfation could guide the virus towards the cell surface. During this process, the mucin-like structures of HSV glycoproteins could be of importance to prevent premature trapping of the virus. Once it reached the cell surface, the virus could continue diffusing along the surface until it reaches a suitable site for cellular uptake, maybe inducing a reorganization of viral glycoproteins that leads to the formation of strong irreversible bonds with membrane receptors, strongly confining the virion. The above described HSV infection pathway remains hypothetical to this point, but could be clarified using live-cell imaging, in complement with the cell membrane mimics described in this thesis. In particular, cell lines with different GAG expression, as well as nSLBs derived from those cells, could be used to fully decipher the diffusive mechanisms of HSV during cell infection.

Finally, although this thesis work entirely focused on HSV, it is likely that the here-discussed findings are, at least partially, transferable to other virus types. The mere fact that GAGs serve as primary attachment factors for a large number of viruses indicates that viruses belonging to different families can share common infection pathways. This thesis therefore aimed at contributing to one main long-term goal, which is an in-depth understanding of the general viral infection mechanisms, necessary to fight current viral diseases and future epidemics.

Bibliography

[1] International Committee on Taxonomy of Viruses (ICTV) - Master Species List 2017 v1.0. Retrieved from: https://talk.ictvonline.org/files/master-species-lists/m/msl/7185, 2018-04-10.

[2] M. J. Roossinck, "The good viruses: Viral mutualistic symbioses," *Nature Reviews Microbiology*, vol. 9, no. 2, pp. 99–108, 2011.

[3] World Health Organization (WHO) - Ebola Situation Report, 10 June 2016. Retrieved from: http://www.who.int/csr/disease/ebola/en/, 2018-04-10.

[4] K. N. Bossart, D. L. Fusco, and C. C. Broder, *Viral Entry into Host Cells*. Springer, 2013.

[5] S. Olofsson and T. Bergström, "Glycoconjugate glycans as viral receptors," *Annals of Medicine*, vol. 37, no. 3, pp. 154–172, 2005.

[6] R. J. Whitley and B. Roizman, "Herpes simplex virus infections," *The Lancet*, vol. 357, no. 9267, pp. 1513–1518, 2001.

[7] D. WuDunn and P. G. Spear, "Initial interaction of herpes simplex virus with cells is binding to heparan sulfate," *Journal of Virology*, vol. 63, no. 1, pp. 52–58, 1989.

[8] C. Singer, *A Short History of Anatomy & Physiology from the Greeks to Harvey*. Dover Publications, Inc., 1957.

[9] R. Phillips, J. Kondev, J. Theriot, and H. G. Garcia, *Physical Biology of the Cell*. Garland Science, 2nd ed., 2013.

[10] J. N. Israelachvili, *Intermolecular and Surface Forces*. Elsevier Inc., 3rd ed., 2011.

[11] B. Kronberg, K. Holmberg, and B. Lindman, *Surface Chemistry of Surfactants and Polymers*. Wiley, 2014.

[12] B. Alberts, A. Johnson, and J. Lewis, *Molecular Biology of the Cell*. Garland Publishing Inc., 5th ed., 2007.

[13] S. J. J. Singer and G. L. L. Nicolson, "The fluid mosaic model of the structure of cell membranes," *Science*, vol. 175, no. 4023, pp. 720–731, 1972.

[14] J.-F. Tocanne, L. Dupou-Cézanne, and A. Lopez, "Lateral diffusion of lipids in model and natural membranes," *Progress in Lipid Research*, vol. 33, no. 3, pp. 203–237, 1994.

[15] M. J. Saxton and K. Jacobsson, "Single-particle tracking: Applications to membrane dynamics," *Annual review of biophysics and biomolecular structure*, vol. 26, pp. 373–399, 1997.

[16] M. J. Karnovsky, a. M. Kleinfeld, R. L. Hoover, and R. D. Klausner, "The concept of lipid domains in membranes," *The Journal of cell biology*, vol. 94, no. 1, pp. 1–6, 1982.

[17] D. A. Brown and E. London, "Structure and function of sphingolipid- and cholesterol-rich membrane rafts," *Journal of Biological Chemistry*, vol. 275, no. 23, pp. 17221–17224, 2000.

[18] J. Riethmüller, A. Riehle, H. Grassmé, and E. Gulbins, "Membrane rafts in host-pathogen interactions," *Biochimica et Biophysica Acta - Biomembranes*, vol. 1758, no. 12, pp. 2139–2147, 2006.

[19] V. Michel and M. Bakovic, "Lipid rafts in health and disease," *Biology of the Cell*, vol. 99, no. 3, pp. 129–140, 2007.

[20] M. L. Kraft, "Plasma membrane organization and function: moving past lipid rafts," *Molecular Biology of the Cell*, vol. 24, no. 18, pp. 2765–2768, 2013.

[21] S. Mañes, G. Del Real, and C. Martínez-A, "Pathogens: Raft hijackers," *Nature Reviews Immunology*, vol. 3, no. 7, pp. 557–568, 2003.

[22] N. Chazal and D. Gerlier, "Virus Entry, Assembly, Budding, and Membrane Rafts," *Microbiology and Molecular Biology Reviews*, vol. 67, no. 2, pp. 226–237, 2003.

[23] Y. Cheng, M. Li, S. Wang, H. Peng, S. Reid, N. Ni, H. Fang, W. Xu, and B. Wang, "Carbohydrate biomarkers for future disease detection and treatment," *Science China Chemistry*, vol. 53, no. 1, pp. 3–20, 2010.

[24] R. Apweiler, H. Hermjakob, and N. Sharon, "On the frequency of protein glycosylation, as deduced from analysis of the SWISS-PROT database," *Biochimica et Biophysica Acta - General Subjects*, vol. 1473, no. 1, pp. 4–8, 1999.

[25] A. M. Meledeo, V. D. Paruchuri, J. Du, Z. Wang, and K. J. Yarema, "Mammalian Glycan Biosynthesis: Building a Template for Biological Recognition," in *Carbohydrate Recognition: Biological Problems, Methods and Applications*, ch. 1, Wiley, 2011.

[26] I. Fernaud-Espinosa, M. Nieto-Sampedro, and P. Bovolenta, "Developmental distribution of glycosaminoglycans in embryonic rat brain: Relationship to axonal tract formation," *Journal of Neurobiology*, vol. 30, no. 3, pp. 410–424, 1996.

[27] R. Sasisekharan, Z. Shriver, G. Venkataraman, and U. Narayanasami, "Roles of heparan-sulphate glycosaminoglycans in cancer," *Nature reviews. Cancer*, vol. 2, no. 7, pp. 521–528, 2002.

[28] T. Uyama, M. Ishida, T. Izumikawa, E. Trybala, F. Tufaro, T. Bergström, K. Sugahara, and H. Kitagawa, "Chondroitin 4-O-sulfotransferase-1 regulates E disaccharide expression of chondroitin sulfate required for herpes simplex virus infectivity," *Journal of Biological Chemistry*, vol. 281, no. 50, pp. 38668–38674, 2006.

[29] C. I. Gama and L. C. Hsieh-Wilson, "Chemical approaches to deciphering the glycosaminoglycan code," *Current Opinion in Chemical Biology*, vol. 9, no. 6, pp. 609–619, 2005.

[30] J. D. Esko, K. Kimata, and U. Lindahl, "Proteoglycans and Sulfated Glycosaminoglycans," in *Essentials of Glycobiology*, ch. 16, Cold Spring Harbor Laboratory Press, 2 ed., 2009.

[31] L. J. Stöh and T. Stehle, "Glycan Engagement by Viruses: Receptor Switches and Specificity," *Annual Review of Virology*, vol. 1, no. 1, p. 140707224641009, 2013.

[32] W. Weis, J. H. Brown, S. Cusack, J. C. Paulson, J. J. Skehel, and D. C. Wiley, "Structure of the influenza virus haemagglutinin complexed with its receptor, sialic acid," *Nature*, vol. 333, no. 6172, pp. 426–431, 1988.

[33] A. C. S. Saphire, M. D. Bobardt, Z. Zhang, P. A. Gallay, Z. H. E. Zhang, and G. David, "Syndecans Serve as Attachment Receptors for Human Immunodeficiency Virus Type 1 on Macrophages," *Journal of Virology*, vol. 75, no. 19, pp. 9187–9200, 2001.

[34] B. Salvador, N. R. Sexton, R. Carrion, J. Nunneley, J. L. Patterson, I. Steffen, K. Lu, M. O. Muench, D. Lembo, and G. Simmons, "Filoviruses utilize glycosaminoglycans for their attachment to target cells," *Journal of Virology*, vol. 87, no. 6, pp. 3295–304, 2013.

[35] S. Y. Kim, J. Zhao, X. Liu, K. Fraser, L. Lin, X. Zhang, F. Zhang, J. S. Dordick, and R. J. Linhardt, "Interaction of Zika Virus Envelope Protein with Glycosaminoglycans," *Biochemistry*, vol. 56, pp. 1151–1162, 2017.

[36] T. Giroglou, L. Florin, F. Schafer, R. Streeck, and M. Sapp, "Human Papillomavirus Infection Requires Cell Surface Heparan Sulfate," *Journal of Virology*, vol. 75, no. 3, pp. 1565 – 1570, 2001.

[37] D. R. Harper, *Viruses: Biology, Applications and Control*. Garland Science, 2012.

[38] J. Carter and V. Saunders, *Virology: Principles and Applications*. Wiley, 2007.

[39] D. W. White, R. Suzanne Beard, and E. S. Barton, "Immune modulation during latent herpesvirus infection," *Immunological Reviews*, vol. 245, no. 1, pp. 189–208, 2012.

[40] W. E. Lafferty, R. W. Coombs, J. Benedetti, C. Critchlow, and L. Corey, "Recurrences after oral and genital herpes simplex virus infection. Influence of site of infection and viral type," *The New England journal of medicine*, vol. 316, no. 23, pp. 1444–9, 1987.

[41] World Health Organization (WHO): Herpes simplex virus. Retrieved from: http://www.who.int/mediacentre/factsheets/fs400/en/, 2018-02-06.

[42] D. J. McGeoch, M. A. Dalrymple, A. J. Davison, A. Dolan, M. C. Frame, D. McNab, L. J. Perry, J. E. Scott, and P. Taylor, "The complete DNA sequence of the long unique region in the genome of herpes simplex virus type 1," *Journal of General Virology*, vol. 69, no. 7, pp. 1531–1574, 1988.

[43] A. Dolan, F. E. Jamieson, C. Cunningham, B. C. Barnett, and D. J. McGeoch, "The genome sequence of herpes simplex virus type 2," *Journal of Virology*, vol. 72, no. 3, pp. 2010–2021, 1998.

[44] C. G. Handler and R. J. Eisenberg, "Oligomeric structure of glycoproteins in herpes simplex virus type 1," *Journal of Virology*, vol. 70, no. 9, pp. 6067–6075, 1996.

[45] B. C. Herold, D. WuDunn, N. Soltys, and P. G. Spear, "Glycoprotein C of herpes simplex virus type 1 plays a principal role in the adsorption of virus to cells and in infectivity," *Journal of Virology*, vol. 65, no. 3, pp. 1090–8, 1991.

[46] B. W. Banfield, Y. Leduc, L. Esford, R. J. Visalli, C. R. Brandt, and F. Tufaro, "Evidence for an Interaction of Herpes Simplex Virus with Chondroitin Sulfate Proteoglycans during Infection," *Virology*, vol. 208, pp. 531–539, 1995.

[47] K. Mårdberg, E. Trybala, F. Tufaro, and T. Bergström, "Herpes simplex virus type 1 glycoprotein C is necessary for efficient infection of chondroitin sulfate-expressing gro2C cells," *Journal of General Virology*, vol. 83, no. 2, pp. 291–300, 2002.

[48] B. C. Herold, R. J. Visalli, N. Susmarski, C. R. Brandt, and P. G. Spear, "Glycoprotein C-independent binding of herpes simplex virus to cells requires cell surface heparan sulphate and glycoprotein B," *Journal of General Virology*, vol. 75, no. 6, pp. 1211–1222, 1994.

[49] S. I. Gerber, B. J. Belval, and B. C. Herold, "Differences in the role of glycoprotein C of HSV-1 and HSV-2 in viral binding may contribute to serotype differences in cell tropism," *Virology*, vol. 214, no. 1, pp. 29–39, 1995.

[50] N. Cheshenko and B. C. Herold, "Glycoprotein B plays a predominant role in mediating herpes simplex virus type 2 attachment and is required for entry and cell-to-cell spread," *Journal of General Virology*, vol. 83, no. 9, pp. 2247–2255, 2002.

[51] P. G. Spear, "Herpes simplex virus: Receptors and ligands for cell entry," *Cellular Microbiology*, vol. 6, no. 5, pp. 401–410, 2004.

[52] P. G. Spear, R. J. Eisenberg, and G. H. Cohen, "Three classes of cell surface receptors for alphaherpesvirus entry," *Virology*, vol. 275, no. 1, pp. 1–8, 2000.

[53] A. V. Nicola, A. M. Mcevoy, and S. E. Straus, "Roles for Endocytosis and Low pH in Herpes Simplex Virus Entry into HeLa and Chinese Hamster Ovary Cells," *Allergy*, vol. 77, no. 9, pp. 5324–5332, 2003.

[54] G. M. Air and W. G. Laver, "The neuraminidase of influenza virus," *Proteins: Structure, Function and Genetics*, vol. 6, no. 4, pp. 341–356, 1989.

[55] S. R. Hadigal, A. M. Agelidis, G. a. Karasneh, T. E. Antoine, A. M. Yakoub, V. C. Ramani, A. R. Djalilian, R. D. Sanderson, and D. Shukla, "Heparanase is a host enzyme required for herpes simplex virus-1 release from cells," *Nature Communications*, pp. 1–11, 2015.

[56] R. Datema, S. Olofsson, and P. A. Romero, "Inhibitors of protein glycosylation and glycoprotein processing in viral systems," *Pharmacology & Therapeutics*, vol. 33, no. 2-3, pp. 221–286, 1987.

[57] D. J. Vigerust and V. L. Shepherd, "Virus glycosylation: role in virulence and immune interactions," *Trends in Microbiology*, vol. 15, no. 5, pp. 211–218, 2007.

[58] S. Olofsson and J.-E. S. Hansen, "Host cell glycosylation of viral glycoproteins - A battlefield for host defence and viral resistance," *Scandinavian Journal of Infectious Diseases*, vol. 30, no. 5, 1998.

[59] A. H. Rux, W. T. Moore, J. D. Lambris, W. R. Abrams, C. Peng, H. M. Friedman, G. H. Cohen, and R. J. Eisenberg, "Disulfide bond structure determination and biochemical analysis of glycoprotein C from herpes simplex virus," *Journal of Virology*, vol. 70, no. 8, pp. 5455–5465, 1996.

[60] A. H. Rux, H. Lou, J. D. Lambris, H. M. Friedman, R. J. Eisenberg, and G. H. Cohen, "Kinetic analysis of glycoprotein C of herpes simplex virus types 1 and 2 binding to heparin, heparan sulfate, and complement component C3b," *Virology*, vol. 294, no. 2, pp. 324–32, 2002.

[61] R. J. Goldberg, "A Theory of Antibody-Antigen Reactions. I. Theory for Reactions of Multivalent Antigen with Bivalent and Univalent Antibody," *Journal of the American Chemical Society*, vol. 74, no. 22, pp. 5715–5725, 1952.

[62] M. Mammen, S. K. Choi, and G. M. Whitesides, "Polyvalent interactions in biological systems: Implications for design and use of multivalent ligands and inhibitors," *Angewandte Chemie-International Edition*, vol. 37, no. 20, pp. 2755–2794, 1998.

[63] V. P. Zhdanov, "Multivalent ligand-receptor-mediated interaction of small filled vesicles with a cellular membrane," *Physical Review E*, vol. 96, no. 1, pp. 1–10, 2017.

[64] P. Kukura, H. Ewers, C. Müller, A. Renn, A. Helenius, and V. Sandoghdar, "High-speed nanoscopic tracking of the position and orientation of a single virus," *Nature methods*, vol. 6, no. 12, pp. 923–927, 2009.

[65] H. Ewers, V. Jacobsen, E. Klotzsch, A. E. Smith, A. Helenius, and V. Sandoghdar, "Label-free optical detection and tracking of single virions bound to their receptors in supported membrane bilayers," *Nano Letters*, vol. 7, no. 8, pp. 2263–2266, 2007.

[66] O. M. Szklarczyk, N. González-Segredo, P. Kukura, A. Oppenheim, D. Choquet, V. Sandoghdar, A. Helenius, I. F. Sbalzarini, and H. Ewers, "Receptor Concentration and Diffusivity Control Multivalent Binding of Sv40 to Membrane Bilayers," *PLoS Computational Biology*, vol. 9, no. 11, pp. 1–16, 2013.

[67] D. Baram-Pinto, S. Shukla, A. Gedanken, and R. Sarid, "Inhibition of HSV-1 attachment, entry, and cell-to-cell spread by functionalized multivalent gold nanoparticles," *Small*, vol. 6, no. 9, pp. 1044–1050, 2010.

[68] E. Rothenberg, L. A. Sepúlveda, S. O. Skinner, L. Zeng, P. R. Selvin, and I. Golding, "Single-virus tracking reveals a spatial receptor-dependent search mechanism," *Biophysical Journal*, vol. 100, no. 12, pp. 2875–2882, 2011.

[69] V. Schubertová, F. J. Martinez-Veracoechea, and R. Vácha, "Influence of ligand distribution on uptake efficiency," *Soft Matter*, vol. 11, no. 14, pp. 2726–2730, 2015.

[70] A. B. Dahlin, "Kinetics of Molecular Binding to Surfaces," in *Plasmonic Biosensors - An Integrated View of Refractometric Detection*, ch. 3, IOA Press, 2012.

[71] A. V. Hill, "The Combinations of Haemoglobin with Oxygen and with Carbon Monoxide," *Biochemical Journal*, vol. 7, no. 1, pp. 471–480, 1913.

[72] J. N. Weiss, "The Hill equation revisited: uses and misuses," *The FASEB journal : official publication of the Federation of American Societies for Experimental Biology*, vol. 11, no. 11, pp. 835–841, 1997.

[73] A. Gunnarsson, P. Jönsson, R. Marie, J. O. Tegenfeldt, and F. Höök, "Single-molecule detection and mismatch discrimination of unlabeled DNA targets," *Nano Letters*, vol. 8, no. 1, pp. 183–188, 2008.

[74] A. Einstein, "Über die von der molekularkinetischen Theorie der Wärme geforderte Bewegung von in ruhenden Flüssigkeiten suspendierten Teilchen," *Annalen der Physik*, vol. 332, no. 8, pp. 549–560, 1905.

[75] R. A. Dragovic, C. Gardiner, A. S. Brooks, D. S. Tannetta, D. J. P. Ferguson, P. Hole, B. Carr, C. W. G. Redman, A. L. Harris, P. J. Dobson, P. Harrison, and I. L. Sargent, "Sizing and phenotyping of cellular vesicles using Nanoparticle Tracking Analysis," *Nanomedicine: Nanotechnology, Biology, and Medicine*, vol. 7, no. 6, pp. 780–788, 2011.

[76] A. Yildiz, "Myosin V Walks Hand-Over-Hand: Single Fluorophore Imaging with 1.5-nm Localization," *Science*, vol. 300, no. 5628, pp. 2061–2065, 2003.

[77] J. Yguerabide, J. A. Schmidt, and E. E. Yguerabide, "Lateral mobility in membranes as detected by fluorescence recovery after photobleaching," *Biophysical journal*, vol. 40, no. 1, pp. 69–75, 1982.

[78] T. K. L. Meyvis, S. C. De Smedt, P. Van Oostveldt, and J. Demeester, "Fluorescence recovery after photobleaching: A versatile tool for mobility and interaction

measurements in pharmaceutical research," *Pharmaceutical Research*, vol. 16, no. 8, pp. 1153–1162, 1999.

[79] P. Jönsson, M. P. Jonsson, J. O. Tegenfeldt, and F. Höök, "A method improving the accuracy of fluorescence recovery after photobleaching analysis," *Biophysical journal*, vol. 95, no. 11, pp. 5334–5348, 2008.

[80] N. Ruthardt, D. C. Lamb, and C. Bräuchle, "Single-particle tracking as a quantitative microscopy-based approach to unravel cell entry mechanisms of viruses and pharmaceutical nanoparticles," *Molecular therapy : the journal of the American Society of Gene Therapy*, vol. 19, no. 7, pp. 1199–211, 2011.

[81] C. Bertucci, S. Cimitan, and L. Menotti, "Optical biosensor analysis in studying herpes simplex virus glycoprotein D binding to target nectin1 receptor," *Journal of Pharmaceutical and Biomedical Analysis*, vol. 32, no. 4-5, pp. 697–706, 2003.

[82] T. Takahashi, S. Kawagishi, M. Masuda, and T. Suzuki, "Binding kinetics of sulfatide with influenza a virus hemagglutinin," *Glycoconjugate Journal*, vol. 30, no. 7, pp. 709–716, 2013.

[83] S. Pustylnikov, R. S. Dave, Z. K. Khan, V. Porkolab, A. A. Rashad, M. Hutchinson, F. Fieschi, I. Chaiken, and P. Jain, "Short Communication: Inhibition of DC-SIGN-Mediated HIV-1 Infection by Complementary Actions of Dendritic Cell Receptor Antagonists and Env-Targeting Virus Inactivators," *AIDS Research and Human Retroviruses*, vol. 32, no. 1, pp. 93–100, 2016.

[84] C. F. Shuman, M. D. Hämäläinen, and U. H. Danielson, "Kinetic and thermodynamic characterization of HIV-1 protease inhibitors," *Journal of molecular recognition : JMR*, vol. 17, no. 2, pp. 106–119, 2004.

[85] D. Massotte, "G protein-coupled receptor overexpression with the baculovirus-insect cell system: A tool for structural and functional studies," *Biochimica et Biophysica Acta - Biomembranes*, vol. 1610, no. 1, pp. 77–89, 2003.

[86] A. M. Seddon, P. Curnow, and P. J. Booth, "Membrane proteins, lipids and detergents: Not just a soap opera," *Biochimica et Biophysica Acta - Biomembranes*, vol. 1666, no. 1-2, pp. 105–117, 2004.

[87] P. Stenlund, G. J. Babcock, J. Sodroski, and D. G. Myszka, "Capture and reconstitution of G protein-coupled receptors on a biosensor surface," *Analytical Biochemistry*, vol. 316, no. 2, pp. 243–250, 2003.

[88] U. Bilitewski, "Protein-sensing assay formats and devices," *Analytica Chimica Acta*, vol. 568, no. 1-2, pp. 232–247, 2006.

[89] B. Prieto-Simín, M. Campàs, and J.-L. Marty, "Biomolecule immobilization in biosensor development: tailored strategies based on affinity interactions," *Protein and peptide letters*, vol. 15, no. 8, pp. 757–763, 2008.

[90] G. L. Kenausis, J. Vörös, D. L. Elbert, N. Huang, R. Hofer, L. Ruiz-Taylor, M. Textor, J. A. Hubbell, and N. D. Spencer, "Poly(L-lysine)-g-Poly(ethylene glycol) Layers on Metal Oxide Surfaces: Attachment Mechanism and Effects of Polymer Architecture on Resistance to Protein Adsorption," *The Journal of Physical Chemistry B*, vol. 104, no. 14, pp. 3298–3309, 2000.

[91] B. Sweryda-Krawiec, H. Devaraj, G. Jacob, and J. J. Hickman, "A New Interpretation of Serum Albumin Surface Passivation," *Langmuir*, vol. 20, no. 6, pp. 2054–2056, 2004.

[92] R. Phillips, T. Ursell, P. Wiggins, and P. Sens, "Emerging roles for lipids in shaping membrane-protein function," *Nature*, vol. 459, no. 7245, pp. 379–385, 2009.

[93] W. Dowhan and M. Bogdanov, "Lipid–protein interactions as determinants of membrane protein structure and function," *Biochemical Society*, vol. 39, no. 3, pp. 767–774, 2011.

[94] C. M. Steffens and T. J. Hope, "Mobility of the Human Immunodeficiency Virus (HIV) Receptor CD4 and Coreceptor CCR5 in Living Cells : Implications for HIV Fusion and Entry Events," *Journal of Virology*, vol. 78, no. 17, pp. 9573–9578, 2004.

[95] J. M. Johnson, T. Ha, S. Chu, and S. G. Boxer, "Early steps of supported bilayer formation probed by single vesicle fluorescence assays," *Biophysical Journal*, vol. 83, no. 6, pp. 3371–3379, 2002.

[96] R. P. Richter, R. Bérat, and A. R. Brisson, "Formation of solid-supported lipid bilayers: An integrated view," *Langmuir*, vol. 22, no. 8, pp. 3497–3505, 2006.

[97] L. Tamm and H. McConnell, "Supported phospholipid bilayers," *Biophysical Journal*, vol. 47, no. 1, pp. 105–113, 1985.

[98] T. H. Anderson, Y. Min, K. L. Weirich, H. Zeng, D. Fygenson, and J. N. Israelachvili, "Formation of supported bilayers on silica substrates," *Langmuir*, vol. 25, no. 12, pp. 6997–7005, 2009.

[99] F. Persson, J. Fritzsche, K. U. Mir, M. Modesti, F. Westerlund, and J. O. Tegenfeldt, "Lipid-based passivation in nanofluidics," *Nano Letters*, vol. 12, no. 5, pp. 2260–2265, 2012.

[100] M. Bally, G. E. Rydell, R. Zahn, W. Nasir, C. Eggeling, M. E. Breimer, L. Svensson, F. Höök, and G. Larson, "Norovirus GII.4 virus-like particles recognize galactosylceramides in domains of planar supported lipid bilayers," *Angewandte Chemie*, vol. 51, no. 48, pp. 12020–4, 2012.

[101] D. W. Lee, H. L. Hsu, K. B. Bacon, and S. Daniel, "Image restoration and analysis of influenza virions binding to membrane receptors reveal adhesion-strengthening kinetics," *PLoS ONE*, vol. 11, no. 10, pp. 1–27, 2016.

[102] H.-L. Hsu, J. K. Millet, D. A. Costello, G. R. Whittaker, and S. Daniel, "Viral fusion efficacy of specific H3N2 influenza virus reassortant combinations at single-particle level," *Scientific Reports*, vol. 6, no. 1, p. 35537, 2016.

[103] D. A. Costello, D. W. Lee, J. Drewes, K. A. Vasquez, K. Kisler, U. Wiesner, L. Pollack, G. R. Whittaker, and S. Daniel, "Influenza virus-membrane fusion triggered by proton uncaging for single particle studies of fusion kinetics," *Analytical Chemistry*, vol. 84, no. 20, pp. 8480–8489, 2012.

[104] L. Simonsson and F. Höök, "Formation and Diffusivity Characterization of Supported Lipid Bilayers with Complex Lipid Compositions," *Langmuir*, vol. 28, pp. 10528–10533, 2012.

[105] G. J. Hardy, R. Nayak, S. M. Alam, J. G. Shapter, F. Heinrich, S. Zauscher, S. Munir Alam, J. G. Shapter, F. Heinrich, and S. Zauscher, "Biomimetic supported lipid bilayers with high cholesterol content formed by α-helical peptide-induced vesicle fusion," *Journal of Materials Chemistry*, vol. 22, no. 37, p. 19506, 2012.

[106] K. Grillitsch, P. Tarazona, L. Klug, T. Wriessnegger, G. Zellnig, E. Leitner, I. Feussner, and G. Daum, "Isolation and characterization of the plasma membrane from the yeast Pichia pastoris," *Biochimica et biophysica acta*, vol. 1838, no. 7, pp. 1889–97, 2014.

[107] M. Tanaka, F. F. Rossetti, and S. Kaufmann, "Native supported membranes: Creation of two-dimensional cell membranes on polymer supports (Review)," *Biointerphases*, vol. 3, no. 2, pp. FA12–FA16, 2008.

[108] R. Scott, "Plasma membrane vesiculation: a new technique for isolation of plasma membranes," *Science*, vol. 194, no. 4266, pp. 743–745, 1976.

[109] M. J. Richards, C.-Y. Hsia, R. R. Singh, H. Haider, J. Kumpf, T. Kawate, and S. Daniel, "Membrane Protein Mobility and Orientation Preserved in Supported Bilayers Created Directly from Cell Plasma Membrane Blebs," *Langmuir*, vol. 32, no. 12, pp. 2963–2974, 2016.

[110] A. Granéli, J. Rydström, B. Kasemo, and F. Höök, "Formation of Supported Lipid Bilayer Membranes on SiO2 from Proteoliposomes Containing Transmembrane Proteins," *Langmuir*, vol. 19, no. 3, pp. 842–850, 2003.

[111] M. Sundh, S. Svedhem, and D. S. Sutherland, "Influence of phase separating lipids on supported lipid bilayer formation at SiO2 surfaces," *Physical chemistry chemical physics : PCCP*, vol. 12, no. 2, pp. 453–60, 2010.

[112] G. J. Hardy, R. Nayak, and S. Zauscher, "Model cell membranes: Techniques to form complex biomimetic supported lipid bilayers via vesicle fusion," *Curr Opin Colloid Interface Sci.*, vol. 18, no. 5, pp. 448–458, 2013.

[113] L. Simonsson, A. Gunnarsson, P. Wallin, P. Jönsson, and F. Höök, "Continuous lipid

bilayers derived from cell membranes for spatial molecular manipulation," *Journal of the American Chemical Society*, vol. 133, no. 35, pp. 14027–14032, 2011.

[114] D. A. Costello, C. Y. Hsia, J. K. Millet, T. Porri, and S. Daniel, "Membrane fusion-competent virus-like proteoliposomes and proteinaceous supported bilayers made directly from cell plasma membranes," *Langmuir*, vol. 29, no. 21, pp. 6409–6419, 2013.

[115] C. E. Dodd, B. R. G. Johnson, L. J. C. Jeuken, T. D. H. Bugg, R. J. Bushby, and S. D. Evans, "Native E. coli inner membrane incorporation in solid-supported lipid bilayer membranes," *Biointerphases*, vol. 3, no. 2, pp. FA59–FA67, 2008.

[116] H. Y. Liu, W. L. Chen, C. K. Ober, and S. Daniel, "Biologically Complex Planar Cell Plasma Membranes Supported on Polyelectrolyte Cushions Enhance Transmembrane Protein Mobility and Retain Native Orientation," *Langmuir*, vol. 34, no. 3, pp. 1061–1072, 2018.

[117] D. A. Costello, J. K. Millet, C. Y. Hsia, G. R. Whittaker, and S. Daniel, "Single particle assay of coronavirus membrane fusion with proteinaceous receptor-embedded supported bilayers," *Biomaterials*, vol. 34, no. 32, pp. 7895–7904, 2013.

[118] H. Pace, L. Simonsson Nyström, A. Gunnarsson, E. Eck, C. Monson, S. Geschwindner, A. Snijder, and F. Höök, "Preserved Transmembrane Protein Mobility in Polymer-Supported Lipid Bilayers Derived from Cell Membranes," *Analytical Chemistry*, vol. 87, no. 18, pp. 9194–9203, 2015.

[119] P. D. Cooper, "The Plaque Assay of Animal Viruses," in *Methods in Virology*, vol. 3, ch. 6, Elsevier Inc., 1967.

[120] R. Dulbecco and M. Vogt, "Some problems of animal virology as studied by the plaque technique," *Cold Spring Harbor symposia on quantitative biology*, vol. 18, pp. 273–279, 1953.

[121] G. Andrei, R. Snoeck, P. Goubau, J. Desmyter, and E. De Clercq, "Comparative Activity of Various Compounds against Clinical Strains of Herpes Simplex Virus," *European Journal of Clinical Microbiology & Infectious Diseases*, vol. 11, no. 2, pp. 143–151, 1992.

[122] K. Nyberg, M. Ekblad, T. Bergström, C. Freeman, C. R. Parish, V. Ferro, and E. Trybala, "The low molecular weight heparan sulfate-mimetic, PI-88, inhibits cell-to-cell spread of herpes simplex virus," *Antiviral Research*, vol. 63, no. 1, pp. 15–24, 2004.

[123] B. Brandenburg and X. Zhuang, "Virus trafficking - learning from single-viruses tracking," *Nat Rev Microbiol.*, vol. 5, no. 3, pp. 197–208, 2007.

[124] Y.-F. Huang, G.-Y. Zhuo, C.-Y. Chou, C.-H. Lin, W. Chang, and C.-L. Hsieh, "Coherent Brightfield Microscopy Provides the Spatiotemporal Resolution To Study Early Stage Viral Infection in Live Cells," *ACS Nano*, vol. 11, pp. 2575–2585, 2017.

[125] H. M. Van Der Schaar, M. J. Rust, Chen, H. Van Der Ende-Metselaar, J. Wilschut, X. Zhuang, and J. M. Smit, "Dissecting the cell entry pathway of dengue virus by single-particle tracking in living cells," *PLoS Pathogens*, vol. 4, no. 12, 2008.

[126] P. Liu, M. Ridilla, P. Patel, L. Betts, E. Gallichotte, L. Shahidi, N. L. Thompson, and K. Jacobson, "Beyond attachment: Roles of DC-SIGN in dengue virus infection," *Traffic*, vol. 18, no. 4, pp. 218–231, 2017.

[127] Y. Gu, Y. Yang, and Y. Liu, "Imaging early steps of sindbis virus infection by total internal reflection fluorescence microscopy," *Advances in Virology*, vol. 2011, 2011.

[128] T. Sakai, S. I. Nishimura, T. Naito, and M. Saito, "Influenza A virus hemagglutinin and neuraminidase act as novel motile machinery," *Scientific Reports*, vol. 7, p. 45043, 2017.

[129] C. J. Burckhardt, M. Suomalainen, P. Schoenenberger, K. Boucke, S. Hemmi, and U. F. Greber, "Drifting motions of the adenovirus receptor CAR and immobile integrins initiate virus uncoating and membrane lytic protein exposure," *Cell Host and Microbe*, vol. 10, no. 2, pp. 105–117, 2011.

[130] H. Ewers, A. E. Smith, I. F. Sbalzarini, H. Lilie, P. Koumoutsakos, and A. Helenius, "Single-particle tracking of murine polyoma virus-like particles on live cells and artificial membranes," *Proceedings of the National Academy of Sciences*, vol. 102, no. 42, pp. 15110–15115, 2005.

[131] J. M. Smit, B. L. Waarts, R. Bittman, and J. Wilschut, "Liposomes as Target Membranes in the Study of Virus Receptor Interaction and Membrane Fusion," *Methods in Enzymology*, vol. 372, pp. 374–392, 2003.

[132] I. Nunes-Correia, A. Eulálio, S. Nir, N. Düzgünes, J. Ramalho-Santos, and M. C. Pedroso De Lima, "Fluorescent probes for monitoring virus fusion kinetics: Comparative evaluation of reliability," *Biochimica et Biophysica Acta - Biomembranes*, vol. 1561, no. 1, pp. 65–75, 2002.

[133] O. Wahlsten, F. Ulander, B. Agnarsson, D. Midtvedt, M. Henningson, V. P. Zhdanov, and F. Höök, "Quantitative Detection of Biological Nanoparticles in Solution via their Mediation of Colocalization of Fluorescent Liposomes," *submitted*.

[134] B. Liedberg, C. Nylander, and I. Lunström, "Surface plasmon resonance for gas detection and biosensing," *Sensors and Actuators*, vol. 4, no. C, pp. 299–304, 1983.

[135] N. J. de Mol and M. J. Fischer, "Kinetic and thermodynamic analysis of ligand-receptor interactions: SPR applications in drug development," in *Handbook of Surface Plasmon Resonance*, ch. 5, Royal Society of Chemistry, 2008.

[136] S. A. Maier, *Plasmonics: Fundamentals and applications*. Springer, 2007.

[137] B. Liedberg, I. Lundström, and E. Stenberg, "Principles of biosensing with an ex-

tended coupling matrix and surface plasmon resonance," *Sensors and Actuators B: Chemical*, vol. 11, no. 1-3, pp. 63–72, 1993.

[138] E. Kretschmann, "Die Bestimmung optischer Konstanten von Metallen durch Anregung von Oberflächenplasmaschwingungen," *Zeitschrift für Physik*, vol. 241, no. 4, pp. 313–324, 1971.

[139] J. De Feijter, J. Benjamins, and F. Veer, "Ellipsometry as a tool to study the adsorption behavior of syntetic and biopolyers at the air water interface," *Biopolymers*, vol. 17, no. 7, pp. 1759–1772, 1978.

[140] L. S. Jung, C. T. Campbell, T. M. Chinowsky, M. N. Mar, and S. S. Yee, "Quantitative Interpretation of the Response of Surface Plasmon Resonance Sensors to Adsorbed Films," *Langmuir*, vol. 14, no. 19, pp. 5636–5648, 1998.

[141] J. R. Lakowicz, *Principles of fluorescence spectroscopy*. Springer, 3rd ed., 2006.

[142] T. Förster, Z. Energiewanderung, and F. Von, "Zwischenmolekulare Energiewanderung und Fluoreszenz," *Annalen der Physik*, vol. 248, no. 1938, pp. 55–75, 1939.

[143] C. Berney and G. Danuser, "FRET or no FRET: A quantitative comparison," *Biophysical Journal*, vol. 84, no. 6, pp. 3992–4010, 2003.

[144] B. Schuler and W. A. Eaton, "Protein folding studied by single-molecule FRET," *Current Opinion in Structural Biology*, vol. 18, no. 1, pp. 16–26, 2008.

[145] D. K. Struck, D. Hoekstra, and R. E. Pagano, "Use of resonance energy transfer to monitor membrane fusion," *Biochemistry*, vol. 20, no. 14, pp. 4093–4099, 1981.

[146] D. Axelrod, "Cell-substrate Contacts Illuminated by Total-Internal Reflection Fluorescence," *Journal of Cell Biology*, vol. 89, pp. 141–145, 1981.

[147] D. Axelrod, N. Thompson, and T. P. Burghardt, "Total Internal Reflection Fluorescence," *Ann. Rev. Biophysics & Bioengineering*, vol. 13, no. 247-268, 1984.

[148] D. Axelrod, "Total Internal Reflection Fluorescence Microscopy," in *Methods in Cell Biology*, vol. 89, ch. 7, Elsevier Inc., 1 ed., 2008.

[149] G. K. Binnig, "Atomic force microscope and method for imaging surfaces with atomic resolution," 1988. Patent nr.: US4724318A.

[150] Press Release: The 1986 Nobel Prize in Physics. Retrieved from: https://www.nobelprize.org/nobel_prizes/physics/laureates/1986/press.html , 2017-12-13.

[151] Y. F. Dufrêne, "Atomic Force Microscopy , a Powerful Tool in Microbiology," *Journal of Bacteriology*, vol. 184, no. 19, pp. 5205–5213, 2002.

[152] Y. F. Dufrêne, D. Martínez-Martín, I. Medalsy, D. Alsteens, and D. J. Müller, "Multi-

parametric imaging of biological systems by force-distance curve-based AFM," *Nature methods*, vol. 10, no. 9, pp. 847–54, 2013.

[153] A. M. Whited and P. S.-H. Park, "Atomic force microscopy: a multifaceted tool to study membrane proteins and their interactions with ligands," *Biochimica et biophysica acta*, vol. 1838, no. 1 Pt A, pp. 56–68, 2014.

[154] E. M. Puchner and H. E. Gaub, "Force and function: probing proteins with AFM-based force spectroscopy," *Current Opinion in Structural Biology*, vol. 19, no. 5, pp. 605–614, 2009.

[155] D. J. Müller, H. Janovjak, T. Lehto, L. Kuerschner, and K. Anderson, "Observing structure, function and assembly of single proteins by AFM," *Progress in Biophysics and Molecular Biology*, vol. 79, no. 1-3, pp. 1–43, 2002.

[156] Y. F. Drygin, O. A. Bordunova, M. O. Gallyamov, and I. V. Yaminsky, "Atomic force microscopy examination of tobacco mosaic virus and virion RNA," *FEBS Letters*, vol. 425, no. 2, pp. 217–221, 1998.

[157] M. Baclayon, G. J. L. Wuite, and W. H. Roos, "Imaging and manipulation of single viruses by atomic force microscopy," *Soft Matter*, vol. 6, no. 21, p. 5273, 2010.

[158] Y. G. Kuznetsov, C. Xiao, S. Sun, D. Raoult, M. Rossmann, and A. McPherson, "Atomic force microscopy investigation of the giant mimivirus," *Virology*, vol. 404, no. 1, pp. 127–137, 2010.

[159] Y. L. Lyubchenko, A. A. Gall, L. S. Shlyakhtenko, R. E. Harrington, B. L. Jacobs, P. I. Oden, and S. M. Lindsay, "Atomic force microscopy imaging of double stranded DNA and RNA," *Journal of biomolecular structure & dynamics*, vol. 10, no. 3, pp. 589–606, 1992.

[160] C. Bustamante, J. Vesenka, C. L. Tang, W. Rees, M. Guthold, and R. Keller, "Circular DNA molecules imaged in air by scanning force microscopy," *Biochemistry*, vol. 31, no. 1, pp. 22–26, 1992.

[161] B. Cappella and G. Dietler, "Force-distance curves by atomic force microscopy," *Surface Science Reports*, vol. 34, no. 1-3, pp. 1–104, 1999.

[162] R. Barattin and N. Voyer, "Chemical modifications of AFM tips for the study of molecular recognition events," *Chemical Communications*, no. 13, pp. 1513–1532, 2008.

[163] V. T. Moy, E. L. Florin, and H. E. Gaub, "Adhesive forces between ligand and receptor measured by AFM," *Colloids and Surfaces A: Physicochemical and Engineering Aspects*, vol. 93, no. C, pp. 343–348, 1994.

[164] M. Pfreundschuh, D. Alsteens, R. Wieneke, C. Zhang, S. R. Coughlin, R. Tampé, B. K. Kobilka, and D. J. Müller, "Identifying and quantifying two ligand-binding sites

while imaging native human membrane receptors by AFM," *Nature communications*, vol. 6, p. 8857, 2015.

[165] D. Alsteens, M. Pfreundschuh, C. Zhang, P. M. Spoerri, S. R. Coughlin, B. K. Kobilka, and D. J. Müller, "Imaging G protein–coupled receptors while quantifying their ligand-binding free-energy landscape," *Nature Methods*, vol. 12, no. 9, pp. 845–851, 2015.

[166] E. Evans and K. Ritchie, "Dynamic Strength of Moleculer Adhesion Bonds," *Biophysical Journal*, vol. 72, no. April, pp. 1541–1555, 1997.

[167] E. Evans, "Probing the Relation Between Force—Lifetime—and Chemistry in Single Molecular Bonds," *Annual Review of Biophysics and Biomolecular Structure*, vol. 30, no. 1, pp. 105–128, 2001.

[168] R. Merkel, P. Nassoy, A. Leung, K. Ritchie, and E. Evans, "Energy landscapes of receptor-ligand bonds explored with dynamic force spectroscopy," *Nature*, vol. 397, no. 6714, pp. 50–53, 1999.

[169] E. A. Evans and D. A. Calderwood, "Force and bond dynamics in cell adhesion," *Science*, vol. 316, no. 1148, pp. 1148–53, 2007.

[170] D. Alsteens, R. Newton, R. Schubert, D. Martinez-Martin, M. Delguste, B. Roska, and D. J. Müller, "Nanomechanical mapping of first binding steps of a virus to animal cells," *Nature Nanotechnology*, vol. 12, no. 2, pp. 177–183, 2017.

[171] N. Altgärde, E. Nilebäck, L. de Battice, I. Pashkuleva, R. L. Reis, J. Becher, S. Möller, M. Schnabelrauch, and S. Svedhem, "Probing the biofunctionality of biotinylated hyaluronan and chondroitin sulfate by hyaluronidase degradation and aggrecan interaction," *Acta Biomaterialia*, vol. 9, no. 9, pp. 8158–8166, 2013.

[172] E. Migliorini, D. Thakar, R. Sadir, T. Pleiner, F. Baleux, H. Lortat-Jacob, L. Coche-Guerente, and R. P. Richter, "Well-defined biomimetic surfaces to characterize glycosaminoglycan-mediated interactions on the molecular, supramolecular and cellular levels," *Biomaterials*, vol. 35, no. 32, pp. 8903–8915, 2014.

[173] M. Ito, M. Baba, A. Sato, R. Pauwels, E. De Clercq, and S. Shigeta, "Inhibitory effect of dextran sulfate and heparin on the replication of human immunodeficiency virus (HIV) in vitro," *Antiviral Research*, vol. 7, no. 6, pp. 361–367, 1987.

[174] S. Block, V. P. Zhdanov, and F. Höök, "Quantification of multivalent interactions by tracking single biological nanoparticle mobility on a lipid membrane," *Nano Letters*, vol. 16, no. 7, pp. 4382–4390, 2016.

[175] P. R. Smith, I. E. Morrison, K. M. Wilson, N. Fernández, and R. J. Cherry, "Anomalous diffusion of major histocompatibility complex class I molecules on HeLa cells determined by single particle tracking," *Biophysical Journal*, vol. 76, no. 6, pp. 3331–3344, 1999.

[176] M. Ekblad, B. Adamiak, K. Bergefall, H. Nenonen, A. Roth, T. Bergstrom, V. Ferro, and E. Trybala, "Molecular basis for resistance of herpes simplex virus type 1 mutants to the sulfated oligosaccharide inhibitor PI-88," *Virology*, vol. 367, no. 2, pp. 244–252, 2007.

[177] B. Adamiak, M. Ekblad, T. Bergström, V. Ferro, and E. Trybala, "Herpes simplex virus type 2 glycoprotein G is targeted by the sulfated oligo- and polysaccharide inhibitors of virus attachment to cells," *Journal of Virology*, vol. 81, no. 24, pp. 13424–13434, 2007.

[178] S. Boulant, M. Stanifer, and P. Y. Lozach, "Dynamics of virus-receptor interactions in virus binding, signaling, and endocytosis," *Viruses*, vol. 7, no. 6, pp. 2794–2815, 2015.